Frustrated Kondo impurity triangle: A simple model of deconfinement

Elio J. König, Piers Coleman, and Yashar Komijani

Phys. Rev. B **104**, 115103 — Published 3 September 2021

DOI: 10.1103/PhysRevB.104.115103

Frustrated Kondo impurity triangle: a simple model of deconfinement

Elio J. König,[1,2] Piers Coleman,[1,3] and Yashar Komijani[1,4]

[1] *Department of Physics and Astronomy, Center for Materials Theory, Rutgers University, Piscataway, NJ 08854 USA*
[2] *Max Planck Institute for Solid State Research, Heisenbergstr. 1, 70569 Stuttgart, Germany.*
[3] *Department of Physics, Royal Holloway, University of London, Egham, Surrey TW20 0EX, UK*
[4] *Department of Physics, University of Cincinnati, Cincinnati, Ohio 45221-0011, USA*

(Dated: July 6, 2021)

The concepts of deconfinement and topological order are of great current interest for quantum information science and for our understanding of quantum materials. Here, we introduce a simple model of three antiferromagnetically coupled Kondo impurities, a "Kondo triangle", which can be used to further extend the application of these concepts to electronic systems. We show that by tuning the magnetic frustration, the Kondo triangle undergoes a quantum phase transition between two phases of unbroken symmetry, signaling a phase transition beyond the Landau paradigm. We demonstrate that the frustrated "spin liquid" phase is described by a three-channel Kondo fixed point and thus displays an irrational ground state degeneracy. Using an Abrikosov pseudofermion representation this quantum state is categorized by an emergent U(1) gauge field and its projective symmetry group. The gauge theory is deconfining in the sense that a miniature Wilson loop orders and that topological defects (instantons in the gauge field) are expelled. This phase persists in presence of moderate Kondo screening until proliferation of topological defects lead to a quantum phase transition to an unfrustrated Fermi liquid phase. Based on this evidence, we propose that three-channel Kondo phase displays topological order in a similar sense as gapless spin liquids.

I. INTRODUCTION

Recent discoveries in quantum materials have urged us to generalize Landau's notion of broken symmetry by introducing new classes of quantum order without symmetry breaking. The prime example is quantum magnetism in which strong frustration can give rise to quantum spin liquids (QSLs)[1, 2] with fractionalized quasi-particles, new patterns of long-range entanglement and topological order [3]. Similar physics occurs at continuous phase transitions between ordered phases with different symmetries which require a fractionalized description ("deconfined criticality") [4].

These ideas are of particular relevance to doped QSLs in the vicinity of Mott-delocalization, a topic of potential importance for cuprate [5], organic salts [6, 7] and iron-based [8] high-T_c superconductors. A closely related topic, is the interaction of electrons and spin liquids via a Kondo interaction, as in geometrically frustrated heavy fermion compounds, (e.g. CePdAl [9, 10]), transition metal dichalcogenides (e.g. 4Hb-TaS_2 [11]) and in engineered van-der-Waals heterostructures of graphene and $RuCl_3$ [12].

A significant component of this intriguing physics is thought to involve the fractionalization of spins [13, 14] into "spinons", fractionalized particles interacting with an emergent gauge field. Fractionalization is a useful concept if the emergent gauge theory is in the deconfining phase. In (2+1)D compact quantum electrodynamics (QED_3) deconfinement is lost via a proliferation of instantons in the gauge field [15], but the presence of fermions [16–20] counteracts this mechanism allowing for a confinement-deconfinement quantum phase transition. It has been argued that transitions out of spin-liquid phases via partial Mott delocalization, e.g. in heavy-fermion materials, leads to a Fermi surface reconstruction that may be understood in these terms [21–23].

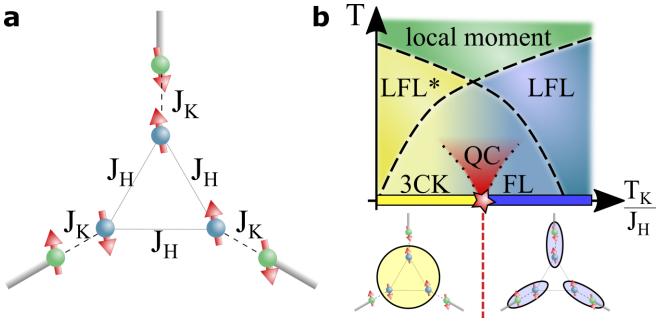

FIG. 1. **a** An antiferromagnetic triangle, where each spin is coupled to its own conduction bath, caricatures a spin-liquid competing with a Fermi liquid. **b** When T_K/J_H is large, each spin is individually Kondo screened (local Fermi liquid LFL, right inset). In contrast, at smallest T_K/J_H, the ground state manifold of the impurity forms an effective spin (left inset) and the system develops a 3 channel Kondo (3CK) phase, in which instantons of the emergent gauge theory are irrelevant. Analogously to confinement in QED_3, instantons proliferate beyond a critical T_K/J_H (red star) and restore an ordinary (L)FL.

In addition to its importance for quantum materials, deconfinement of anyonic quasiparticles is of prime importance for topological quantum computation [24] which may be realized in materials (as discussed above) or by artificially interweaving non-topological qubits into robust, macroscopic logical qubits, e.g. within the surface code. As it appears particularly desirable to *electronically* manipulate and braid the emergent excitations, a natural important question regards when and how topological order is destroyed by the coupling to electronic

leads.

Related phenomena appear in the context of magnetic impurities, as in the overscreened Kondo effect [25–29], and in magnetically frustrated Kondo screened impurities [30–34]. The frustration lead to the fractionalization of the spin and an irrational residual entropy suggestive of an underlying presence of non-Abelian anyons [35]. It has been recently suggested that these anyons can be potentially used as a platform for topological quantum computation [36, 37]. The common theme of these systems is an abundance of competing patterns of spin entanglement and their rearrangement at a quantum critical point (QCP).

Here, we investigate a "Kondo triangle model" involving three antiferromagnetically coupled spins at the vertices of a triangle, each independently coupled to its own conduction sea (Fig. 1 **a**) [38, 39]. The solvable limits of this model enable us to demonstrate a transition between two distinct ground-state phases without any symmetry breaking. In one of these two phases each spin is Kondo screened separately and the spins are not mutually entangled. In the other phase, the spins are strongly entangled, the coupling to the leads results in an irrational impurity entropy. To gain a better insight, we have explored the physics of a Kondo triangle near the large N limit of spins with an SU(N) symmetry. Our procedure contains three steps:

i) We pre-fractionalize spins in terms of Abrikosov fermion "spinons" [40].

ii) Decoupling of interactions leads to a quadratic Hamiltonian [41] with a U(1) flux Φ through the triangle.

iii) We go beyond mean-field theory by studying 1/N corrections and the non-perturbative effects of instantons (i.e. phase-slips $\Phi \to \Phi \pm 2\pi$).

The presence of these phase-slips makes the problem distinct from the two-impurity Kondo problem discussed extensively in the past [28, 42–44] and allows to draw analogies to the confinement mechanism in QED_3 and to fractionalization in 2+1 dimensional quantum materials in general.

We conclude this introduction with an overview of previous works on confinement-deconfinement quantum phase transitions in Kondo lattice systems. Senthil, Vojta and Sachdev [21, 45] introduced the concept of fractionalized Fermi liquid (FL*) phases, in which the Kondo screening of lattice spins breaks down at the expense of establishing a QSL in the spin system. When the latter is a $\mathbb{Z}_2$ QSL, the FL* is particularly robust, but FL* and ordinary Fermi liquid are separated by a superconducting phase which breaks particle number conservation. In contrast, the transition from an FL* with U(1) QSL to the Kondo screened Fermi liquid may be direct, does not involve the breaking of any microscopic symmetries and is governed by a quantum critical point [45–47].To study this phase transition in low-dimensional Kondo problems a study of fermionic degrees of freedom coupled to compact gauge fields seems essential to stabilize deconfinement. We are not aware of any such previous studies.

The remainder of this paper is structured as follows: In Sec. II we define the model under consideration and summarize the main results. Sec. III contains a mapping of the triangle model to a three channel Kondo model which is independent of the approximate large-N treatment introduced in Sec. IV. Fluctuation corrections beyond the $1/N$ limit are discussed in Sec. V while the conclusions, Sec. VI contain a discussion of the relationship to topological order and of the experimental implications of our work.

II. MODEL AND SUMMARY OF RESULTS

A. Model Hamiltonian

The Kondo triangle Hamiltonian (Fig. 1 **a**) $H = H_c + H_{\rm H} + H_{\rm K}$ consists of three terms:

$$H_c = \sum_{m=1}^{3} \sum_{\boldsymbol{p}} \tilde{c}^\dagger_{\alpha,m}(\boldsymbol{p}) \epsilon(\boldsymbol{p}) \tilde{c}_{\alpha,m}(\boldsymbol{p}), \tag{1a}$$

$$H_{\rm H} = \frac{J_H}{N} \sum_{m=1}^{3} \hat{S}^a_m \hat{S}^a_{m+1}, \tag{1b}$$

$$H_{\rm K} = \frac{J_K}{N} \sum_{m=1}^{3} \hat{S}^a_m c^\dagger_{\alpha,m}(0) \sigma^a_{\alpha\beta} c_{\beta,m}(0). \tag{1c}$$

The operators $c^\dagger_m(\boldsymbol{x})$ [$\tilde{c}^\dagger_m(\boldsymbol{p}) = \sum_x e^{-i\boldsymbol{p}\cdot\boldsymbol{x}} c^\dagger_m(\boldsymbol{x})$] create electrons on lead m, with a dispersion $\epsilon(\boldsymbol{p})$. The σ^a ($a = 1 \dots N^2 - 1$) are generators of the fundamental representation of SU(N) and $\hat{S}^a_m$ are the corresponding spin operators. Summation convention over repeated spin indices $\alpha, \beta = 1, \dots, N$ is implied but summations over the lead index m are written explicitly. In this paper, we will mainly use the Abrikosov fermion representation of spins $\hat{S}^a_m = f^\dagger_{\alpha,m}[\sigma^a]_{\alpha\beta} f_{m,\beta}$, with the constraint $f^\dagger_{\alpha,m} f_{\alpha,m} = Q$ where $Q = Nq$.

B. Comparison to previous works

For a large Kondo temperature $T_K = De^{-1/J_K\rho} \gg J_H$ the model yields a local Fermi liquid (LFL), see Fig. 1 **b**, in which each spin is magnetically screened by its own conduction band. The situation is more intricate for small $T_K \ll J_H$. For SU(2) spins, Ferrero *et al.* [38] employed a combination of conformal field theory and numerical renormalization group to demonstrate that the LFL phase is stable at all values of the ratio T_K/J_H. Recently, we investigated the ferromagnetic version [48] of Eq. (1), but we are not aware of other studies of the antiferromagnetic model defined in Eq. (1).

However, C_3 symmetric models of spin-1/2 triangles which are Kondo coupled [49] to a single 2D or 3D electronic bath were considered by Lazarovits *et al.* [32] using a renormalization group approach. Contrary to

Eq. (1), this setup features substantial intersite correlations $\langle c^\dagger_{\alpha,m}(\tau)c_{\alpha,m+1}(0)\rangle$ which can lead to an exotic non-Fermi-liquid fixed point. The model was studied numerically by Paul and Ingersent [50] and analytically by Ingersent *et al.* [30]. Very recently Eickhoff and Anders [51], have re-visited the model with the goal of developing a cluster dynamical mean-field theory.

Finally, a vast amount of literature is devoted to asymmetric triangles, in which Kondo-coupling to the leads is site selective, and/or the Heisenberg interaction is not homogeneous, see e.g. 52–54.

C. Summary of results

In this work, we generalize this model beyond SU(2), to the case of spins forming an antisymmetric representation of SU(N), described by vertical Young tableaux with Q boxes. In Sec. III, we show that for a sequence of (N, Q) our model at smallest T_K/J_H maps onto a single composite spin, overscreened by three conduction channels, denoted here as 3CK. This solvable limit corresponds to a phase with a non-trivial ground state degeneracy, differing from the LFL at large T_K/J_H. Yet, neither phase breaks any symmetries of the model.

Within the large-N approach, the appearance of spinons is accompanied by an emergent $U(1)$ gauge field on the links of the triangle, with a gauge invariant flux $\oint \vec{A}\cdot d\vec{x} = \Phi$ that threads the triangle. The 3CK phase (Fig. 1**b**), is characterized by the ordering of the symmetric ring exchange operator

$$\mathcal{O}_s \equiv d_{abc}\hat{S}^a_1\hat{S}^b_2\hat{S}^c_3 \propto \cos(\Phi), \quad d_{abc} \equiv \mathrm{tr}[\sigma^a\{\sigma^b,\sigma^c\}], \quad (2)$$

which preserves time reversal, spin SU(N) and crystalline C_{3v} symmetries. By contrast, in the Fermi liquid (FL), phase-slips proliferate, confining the spinons to each lead, and in this sense, the two phases are separated by a confinement-deconfinement transition. Both (FL and 3CK) phases are robust against deformations of the triangle (i.e. unequal J_H) which make them suitable for future experimental realizations.

Finally, we comment on special values of Q and N. First, the particle-hole symmetric representation $Q/N = 1/2$, which is related to SU(2) spins, has mean-field solutions for which some of the links are missing and the flux is ill-defined (see Fig. 3 **a**, below). Moreover, the order parameter $\mathcal{O}_s$ of the 3CK phase vanishes for $N = 2$ since $d_{abc} = 0$ for SU(2) spins. These arguments explain the persistence of the FL phase down to $T_K/J_H \to 0$ for the SU(2) triangle [38].

Second, at commensurate representations $Q = N/3$, or $Q = 2N/3$, the spins form a singlet at small T_K/J_H and the competition between Heisenberg and Kondo interactions is analogous to the SU(2) two-impurity two-channel Kondo problem, i.e. the two limiting phases are FLs with conduction electron phase shift of $\delta_c = 0, \pi$. For these commensurate representations, instead of the 3CK phase, we have a FL*, i.e. a gapped spin-liquid which is robust to the Kondo interaction up to a threshold coupling, and a FL* to FL transition.

III. MAPPING TO THREE-CHANNEL-KONDO MODELS

We first highlight a subset of models, with $N = 3Q+1$, of which the simplest is the fundamental representation of $SU(4)$. In these special cases, we can show that three channel Kondo (3CK) behavior develops at large J_H. To see this, we first solve H_H at $J_K = 0$. It is convenient to employ the previously introduced Abrikosov fermion representation of the spin, and we emphasize that here no approximations are made (for details see Appendix A). The antiferromagnetic coupling J_H favors the formation of a maximally antisymmetrized combination of 3Q spinons. Since $3Q = N-1$, this system is one spinon short of an overall SU(N) singlet. Indeed if one of the spins, say m, had a larger representation, i.e. $Q+1$ (rather than Q) vertical boxes, the three spins could form a singlet, denoted by $|\mathrm{singlet}, m\rangle$. When all spins have representation Q, the ground state of the Heisenberg Hamiltonian H_H can be shown (Appendix A 2) to be

$$|\alpha\rangle = \frac{1}{\sqrt{3}}\sum_m f_{m,\alpha}\,|\mathrm{singlet}, m\rangle \quad (3)$$

where $\alpha = 1\ldots N$, and states $\{|\alpha\rangle\}$ form a basis for the conjugate representation of SU(N). The corresponding matrix elements of spin operators in the ground state manifold are given by $\langle\alpha|\hat{S}^a_m|\alpha'\rangle = -\sigma^a_{\alpha',\alpha}$. Since the groundstate of the triangle is given by a spinon hole, it is suggestive to also represent the conduction band in terms of holes $c_{\alpha,m}(\boldsymbol{x}) \to h^\dagger_{\alpha,m}(\boldsymbol{x}), c^\dagger_{\alpha,m}(\boldsymbol{x}) \to h_{\alpha,m}(\boldsymbol{x})$. In the limit of large J_H we thus find a Kondo coupling

$$H_K = \frac{J_K}{N}\sum_{m=1}^{3}[\hat{S}^a]^T h^\dagger_{m,\alpha}(0)[\sigma^a]^T_{\alpha\beta}h_{m,\beta}(0), \quad (4)$$

between the spin and a Fermi sea of holes. Thus at large J_H, the model (1) is equivalent to the 3CK problem in the conjugate representation of SU(N), which is equivalent to the 3CK Kondo model, an exactly solvable model (See Appendix A 2). From this mapping, we know that the ground state has an irrational degeneracy of [55–57]

$$g_N = 1 + 2\cos\left(\frac{2\pi}{N+3}\right). \quad (5)$$

Note that $\lim_{N\to\infty} g_N = 3$. We now develop an approximate field theoretical technique which connects the two limits of the phase diagram, Fig. 1.

IV. LARGE-N TREATMENT

A. Hubbard-Stratonovich decoupling

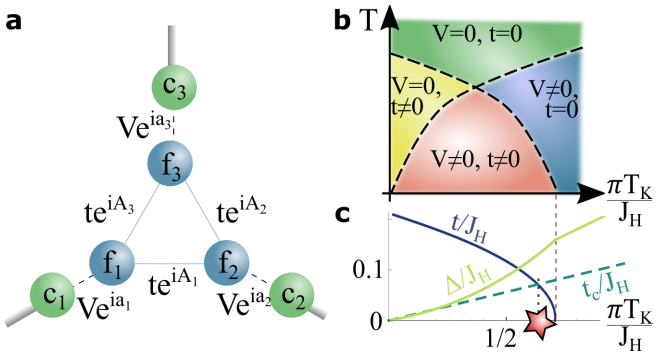

FIG. 2. **a** Pictorial representation of the mean-field Hamiltonian. **b** Schematic mean-field phase diagram. **c** Zero temperature, mean-field behavior of t, $\Delta = \pi\rho V^2$ as a function of Doniach parameter (here $J_4 = 0.3J_H$, $J_s \approx 0.29J_H$). The position where t_c, defined in Eq. (21) below, crosses t defines the confinement-deconfinement quantum phase transition at which phase slips proliferate (red star, here $N = 4$ and $q = 1/4$).

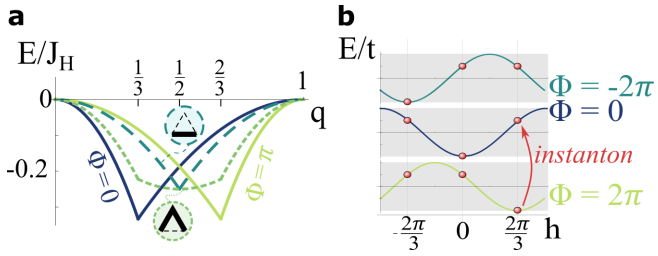

FIG. 3. **a** Ground state energies at $T_K = 0$ as a function of filling q, comparing rotationally symmetric solutions (labeled by their flux Φ) with symmetry broken states with one (two) non-zero t_m [graphically labeled by triangles with one (two) thick bonds]. **b** Single particle spectra of spinons at $T_K = 0$ with helicity quantum numbers $h \in \{0, \pm 2\pi/3\}$ for different flux configurations $\Phi = 0, \pm 2\pi$. Instantons map $\Phi \to \Phi \pm 2\pi$ and thereby reshuffle the wave functions but leave the spectrum unaltered.

Representing the spins using Abrikosov pseudofermions, leads to four-fermion interactions, which we decouple using Hubbard-Stratonovich transformation in the leading channels, selected by the large-N limit (see Fig. 2 **a** for illustration)

$$S = S_c + \int d\tau \sum_m \Big\{ f^\dagger_{\alpha,m}[\partial_\tau + \lambda_m] f_{\alpha,m} - \lambda_m q N + \frac{N|V_m|^2}{J_K} + \frac{N|t_m|^2}{J_H} + [V_m f^\dagger_{\alpha,m} c_{\alpha,m} - t_m f^\dagger_{\alpha,m} f_{\alpha,m+1} + H.c.] \Big\}. \quad (6)$$

Here, $t_m = |t_m| e^{iA_m}$ and $V_m = |V_m| e^{ia_m}$ and the Lagrange multipliers λ_m enforce the constraint (for details, see Appendix B).

B. Mean field solution

1. Mean field Ansätze

In the limit $N \to \infty$, the bosonic path integrals can be evaluated at the saddle point level for static configurations of the fields. At $T_K = V_m = 0$, Fig. 3 **a** demonstrates the stability of homogeneous solutions with $t_m = te^{iA_m}$ and zero or π flux $\Phi = \sum_m A_m$ away from half-filling. In the reverse limit $J_H = t_m = 0$, the equality of Kondo couplings at each of the three sites implies the same hybridization $|V_m|$ for all m. In Read-Newns gauge the phase of V_m is absorbed into λ_m, which also takes the same mean field value at each site. Motivated by this, we concentrate on rotationally symmetric solutions $V_m = V$, $|t_m| = t$ and $\lambda_m = \lambda$, all real, and $q < 1/3$. In this case, the spectrum can be found by Fourier transformation leading to a spinon spectrum $\lambda_h = \lambda - 2t\cos(h + \Phi/3)$, see Fig. 3 **b**. Here, we introduced the helicity $h = 0, \pm 2\pi/3$ (the crystal momentum of the periodic 3-site chain). Using this solution, the fermionic path integral can be taken exactly and leads to a free energy

$$\frac{F}{N} = -T \sum_{\epsilon_n, h} \ln[-G_h^{-1}(\epsilon_n)] e^{i\epsilon_n \eta} + 3\left(\frac{t^2}{J_H} + \frac{\Delta}{\pi\rho J_K} - \lambda q \right), \quad (7)$$

Here, $G_h^{-1}(\epsilon_n) = i\epsilon_n - \lambda_h + i\Delta sgn(\epsilon_n)$ in the wide bandwidth limit where $\Delta = \pi\rho V^2$ is the hybridization energy related to V and the density of states ρ. The variation of the free energy with respect to the parameters Φ, λ, Δ, t leads to a set of mean field equations of which we discuss the solutions below.

2. Finite temperature phase diagram

Before presenting details about these equations at zero temperature, we discuss the finite temperature mean field phase diagram, Fig. 2 **b** (a calculation of mean field transition temperatures is presented in App. B 3).

(i) At the highest temperature, the spinons are decoupled, both from each other ($t = 0$) and from their respective conduction band ($V = 0$), so the impurity spins are neither entangled nor screened. This is characterized by decoupled spins showing Curie susceptibility behavior.

(ii) For $T < T_K$ and large T_K/J_H, all moments are individually screened (LFL), i.e. $t = 0$ but $V > 0$.

(iii) At smallest $T_K/J_H \ll 1$ and finite temperature, $t > 0$ but $V = 0$: here a miniature spin-liquid behavior develops. Since the phase shift for all conduction bands is zero, we denote this phase "LFL*" [21] in Fig. 1 **b**.

(iv) Finally, the mean-field phase n which both $V > 0$ and $t > 0$, which is the focus of the rest of the paper. We will show that there is a deconfinement transition inside this mean field phase.

Next, we derive the mean-field transition between these zero temperature phases to map out the mean-field phase diagram.

3. Zero temperature mean field equations

We now investigate the two zero temperature phases. We readily find that $\Phi = 0$ solves the mean field equations and we concentrate on this solution for $q < 1/2$. It is convenient to replace the three other variational parameters (λ, Δ, t) by $(\delta_0, \delta_{2\pi/3}, t)$, where $\delta_h = \delta_{-h} = \mathrm{arccot}(\lambda_h/\Delta)$ is the phase shift in the helicity channel h. The variation of the free energy with respect to the Lagrange multiplier λ enforces a sum rule

$$3\pi q = \delta_0 + 2\delta_{2\pi/3}, \tag{8a}$$

while the variation with respect to t connects the difference $d = \delta_{2\pi/3} - \delta_0$ of phase shifts with the spinon hopping

$$3\pi t = -J_H d. \tag{8b}$$

Note that $t > 0$ implies $d < 0$. The third saddle point equation follows from the variation of the action with respect to Δ. We exploit the previous equation and obtain

$$\left(\frac{\sin(d)}{d}\frac{\pi T_K}{J_H}\right)^3 = \sin\left(\frac{3\pi q + d}{3}\right)\sin^2\left(\frac{3\pi q - 2d}{3}\right). \tag{8c}$$

Note that there is only one variational parameter, d, in this equation, while q and $\pi T_K/J_H$ are fixed externally. For a graphical solution of Eq. (8c), see Fig. 4. It demonstrates that for $q = 1/3$, a state where both $t \neq 0$ and $V \neq 0$ is never the ground state, while for $q < 1/3$ of prime interest in this work, there is a phase with $t \neq 0$ and $V \neq 0$ which persists to the smallest T_K/J_H and is separated from the LFL by a first-order phase transition (an artifact of the mean-field approach).

C. Symmetries

Here, we summarize the underlying symmetry breaking using the language of conventional phase transitions. We emphasize, however, that no physical symmetry is broken in either 3CK or LFL phase. A parallel discussion in terms the projective symmetry groups is therefore included in Sec. IV E, below.

In the UV ($t = V = 0$), Eq. (6) displays a symmetry $U_f(1)^{\otimes 3} \times U_c(1)^{\otimes 3}$ (i.e. $f_m \to e^{i\phi_m(\tau)} f_m$, $c_m \to e^{i\varphi_m} c_m$), of which $U_f(1)^{\otimes 3}$ is a gauge symmetry. The Kondo effect on each site m ($V_m \neq 0$) breaks the symmetry as $U_f(1)^{\otimes 3} \times U_c(1)^{\otimes 3} \to U_{\mathrm{cf}}(1)^{\otimes 3} \equiv G$ fixing $\varphi_m = \phi_m$ for each spin/bath m separately. The three "Goldstone modes" are eaten by the Lagrange multiplier λ_m within the Read-Newns gauge [58]. Most interesting for the present study is the establishment of a spin liquid, in which $|t| > 0$ fixes $\phi_m = \phi + j(m-1)\frac{2\pi}{3}$ with $j \in \{0, 1, 2\} = \mathbb{Z}_3$. Thus, the remaining symmetry $H = U_{\mathrm{cf}}(1) \times \mathbb{Z}_3$ is generated by the total phase ϕ and the insertion of a total flux of $2\pi j$, i.e. a large gauge transformation which leaves the spectrum unchanged, but re-arranges the eigenstates, Fig. 3 **b**. The symmetry breaking $G \to H$ is apparent within the Landau free energy, which we derived (see Appendix B 4) at $T = 0$, $V > 0$ and small $\bar{t} = |t_m|/T_K$

$$\frac{F}{N} = T_K\left[\alpha \bar{t}^{\,2} - \beta \bar{t}^{\,3}\cos(\Phi) + \gamma \bar{t}^{\,4} + O(\bar{t}^5)\right]. \tag{9}$$

where $\alpha = 3T_K/J_H - \sin(\pi q)/\pi$. The flux $\Phi = \sum_m A_m \in [0, 6\pi)$, but Eq. (9) is 2π periodic in the total flux, pointing to the emergent $\mathbb{Z}_3$ gauge symmetry of the problem.

D. Bilinear coupling and ring exchange

The Landau free energy illustrates the first order nature of the mean-field transition: The cubic term is a consequence of the threefold symmetry of the impurity, and additionally the microscopic parameters in Eq. (1) imply $\gamma < 0$ near the transition, reinforcing the first order behavior. A negative quartic term is typical in the large-N treatments and can be cured by inclusion of a biquadratic interaction [22]

$$H_4 = -\frac{\pi^3 J_4}{2N^3}\sum_m [\hat{S}^a_m \hat{S}^a_{m+1}]^2, \tag{10}$$

leading to $\gamma = 3[J_4 \sin(\pi q)^4/T_K - \sin(3\pi q)]/(2\pi)$. The first order jump is further weakened by the addition of a totally symmetric ring exchange

$$H_3 = -\pi^2 \frac{J_s}{N} d_{abc} \hat{S}^a_1 \hat{S}^b_2 \hat{S}^c_3, \tag{11}$$

so that microscopically $\beta = [\sin(2\pi q) - J_s \sin(\pi q)^3/T_K]/\pi$ after integration of fermions. A similar integration is the origin of the relation $\mathcal{O}_s \sim \cos(\Phi)$ presented in Eq. (2).

Ring exchange terms can be employed to physically access the emergent gauge flux Φ. An adiabatic flux insertion can be achieved by adiabatically tuning $\theta(t)$ in

$$\Delta H(t) = -\frac{J}{N}\left\{d_{abc}\cos\theta(t) + f_{abc}\sin\theta(t)\right\}\hat{S}^a_1 \hat{S}^b_2 \hat{S}^c_3$$

where d_{abc} and f_{abc} are symmetric and antisymmetric structure factors of SU(N). A mean-field decoupling of $H + \Delta H$ leads to $\Delta F \propto -J\cos(\Phi - \theta)$.

E. A study of projective symmetry group

We now return to the emergent gauge invariance in the problem and employ the method of projective symmetry groups (PSGs), introduced [59] to categorize gapless spin liquid states which do not break any microscopic (e.g. crystalline) symmetries. To recapitulate the procedure:

(i) Consider a mean field tight binding model of spinons $f_{\alpha,m}$, in our case Eq. (6). Because spinons carry an emergent gauge charge, mean field tight-binding models which can be transformed into each other by means of a gauge transformation are equivalent.

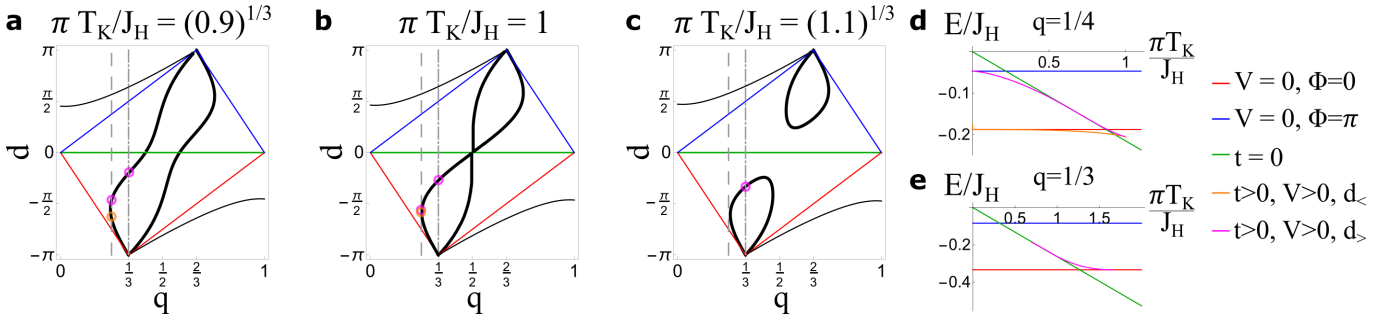

FIG. 4. Graphical illustration of mean field solutions. **a - c** Each point on the black curves corresponds to a solution of Eq. (8c) for a given value of the Doniach parameter $\pi T_K/J_H$. For $q < 1/2$ ($q > 1/2$), we concentrate on $d < 0$ ($d > 0$) (other solutions are "false vacua" indicated as thin lines). For comparison, we include analogous curves of solutions in the limit $T_K = 0$ [$t > 0, V = 0$ (red) and $t < 0, V = 0$ (blue)] as well as $J_H = 0$ [$t = 0, V > 0$ (green)]. The vertical gray dashed lines indicate the position of $q = 1/4, 1/3$. For $q = 1/4$ there are up to two non-trivial solutions with $-\pi < d < 0$ (orange and pink circles, denoted $d_<$ and $d_>$, respectively), while for $q = 1/3$ there is only one non-trivial solution (pink circle) in addition to the solution $d = -\pi$ corresponding to complete Kondo breakdown ($V = 0$). The corresponding mean field energy is plotted with the same color code in **d, e**, and compared to the solutions where either $V = 0$ or $t = 0$.

(ii) The group of microscopic symmetry operations followed by a gauge transformation which leave the tight binding model invariant form the PSG of the model.

(iii) The subgroup of gauge transformations which leave the tight binding Hamiltonian invariant form the invariant gauge group (IGG).

(iv) The actual symmetry group (SG) of the model is thus SG = PSG/IGG. Hence the PSG can be seen as an extension of the SG.

The IGG also places constraints on Wilson loop operators P_C [2], which are products of Peierls gauge fields along closed contours on links of the lattice ($P_C = \prod_{m=1}^{3} e^{iA_m}$ in our simple three-site lattice). Wilson loops are a particularly useful definition for gapless topological quantum states when standard signatures (such as a degenerate ground state manifold) are less obvious.

As mentioned, in our case the infrared gauge transformations are $f_{\alpha,m} \to e^{i\phi_m} f_{\alpha,m}$, $c_{\alpha,m} \to e^{i\phi_m} c_{\alpha,m}$, $A_m \to A_m + \phi_m - \phi_{m+1}$ and imply an IGG which is U(1). The crystalline symmetries group of the triangle is generated by 120° rotations R, $R^3 = 1$ and an involutory mirror operation $M = M^{-1}$ exchanging sites $m = 1 \leftrightarrow m = 2$. They do not commute, instead $MRMR = 1$. We may then proceed with the analysis of the PSG assuming deconfining gauge fields. To projectively represent the rotation, we perform a gauge transformation $f_m \to G_R(m) f_m$, $c_m \to G_R(m) c_m$ with $G_R(m) = e^{iA_m}$ after application of the crystalline symmetry operation. Analogously, the mirror exchanging sites $1 \leftrightarrow 2$ is projectively represented by employing $G_M(m) = e^{i(A_3 - A_2)\delta_{m,3}}$. Since we assume time reversal symmetry, there is a gauge in which all hopping matrix elements are real, i.e. $A_m \in \{0, \pi\}$. Then the algebra of projective symmetry operations is $(G_R R)^3 = e^{i\Phi} = \pm 1$, $(G_M M)^2 = 1$, $(G_M M)(G_R R)(G_M M)(G_R R) = 1$. Thus, the two mean field states associated to $\Phi = 0, \pi$ in Fig. 3 **a** are categorized by different algebraic PSGs. On the mean field level these two states are separated by multiple symmetry broken states - this is reminiscent of the transition between 2D quantum phases with different PSGs coupled to fermionic matter [60].

V. FLUCTUATIONS AND GAUGE FIELDS

In the previous section we discussed the mean field solution to Eq. (1), which is valid at $N = \infty$. Here, we consider fluctuation corrections beyond this limit.

A. Dynamics of low-energy excitations

The bosonic low-energy excitations in the model are the phases A_m, whose action may be derived microscopically by a lengthy but straightforward integration of fermionic degrees of freedom, see Appendix C, leading to $S[A_m] = S_{\rm diss} + S_{\rm Maxwell}$

$$S_{\rm diss} = \int \frac{d\omega}{2\pi} \frac{\eta}{4\pi} \Phi(\omega)\Phi(-\omega)|\omega|, \tag{12a}$$

$$S_{\rm Maxwell} = \int d\tau \sum_m \frac{\epsilon}{2} \dot{A}_m^2, \tag{12b}$$

where

$$\eta \simeq 3N \frac{t^2}{T_K^2} \sin^2(\pi q), \quad (\text{for } t \ll T_K \cos(\pi q)), \tag{13a}$$

$$\epsilon = \frac{2N}{9J_H} \left(1 + \frac{J_H \sin(\delta_{2\pi/3})^2}{2\pi\Delta}\right)(1 + 2\rho\Delta). \tag{13b}$$

Here, we presented the microscopic expression for the low-energy ($|\omega| \ll T_K$) dissipative dynamics of Φ in the limit $t \ll T_K$ (near the QCP, see Fig. 2 **c**). For a more comprehensive expression, see Eq. (C16) of the Appendix.

Before discussing the features of this emergent gauge theory, we analyze the fluctuations using the more conventional language of Goldstone bosons.

B. Goldstone bosons

When $t/t_K > 0$, two combinations of A phases, parametrized by $A_m = -2\vec{x}\cdot\hat{e}_m/3$, where $\hat{e}_{1,2} = (\pm\sqrt{3},1)/2$, $\hat{e}_3 = (0,-1)$, $\vec{x} = (x_1,x_2)$, are zero modes of the free energy Eq. (9) and parametrize the manifold of Goldstone bosons (see Sec. IV C)

$$\frac{G}{H} = \frac{U(1)\times U(1)\times U(1)}{U(1)\times\mathbb{Z}_3}. \tag{14}$$

In contrast, the third linear combination of phases, $\Phi = \sum_m A_m$, is gapped. For $J_H \gg T_K$, the two brackets entering ϵ in Eq. (13b) are approximately one, so we omit them for simplicity. The effective action of Goldstone bosons is thus

$$S_{\text{Goldstone}}[\vec{x}] = \int d\tau \frac{m_x \dot{\vec{x}}^2}{2}, \tag{15}$$

where $m_x = 8N/(27J_H)$. This action describes a free particle with position $\vec{x}$ and mass m_x living on the flat, yet compact manifold (14). The ground state is an $\vec{x}$-independent wave function and, due to the compactness of G/H, detached from the first excited state at energy $\sim 1/m_x$.

As a consequence, despite the mean field value $t>0$, intersite Green's functions $\langle c_m^\dagger c_{m+1}\rangle \sim \langle e^{iA_m}\rangle$ vanish upon integration of Goldstone modes. Therefore, the absence of charge transfer between different leads is ensured by the fluctuations beyond the $N\to\infty$ limit. Equivalently, this can be interpreted as a consequence of gauge symmetry which impedes charge fluctuations on the impurity sites.

C. Confinement-Deconfinement transition

So far, we incorporated leading terms in a $1/N$ series. Now, we address processes with Boltzmann weight $\Gamma \sim e^{-N}$ (instantons). Naively, these are strongly suppressed, yet we demonstrate a proliferation of instantons at sufficiently large T_K/J_H. Instantons in gauge theories are non-trivial gauge field configurations which are bound to be a pure gauge at infinity. In the present case, these are phase slips, i.e. configurations of the field $\Phi(\tau)$ such that $\Phi(\infty)-\Phi(-\infty) = \pm 2\pi$, and we estimate their bare tunneling action $\Gamma \sim e^{-N\bar{t}}$ for $\beta \ll \bar{t}$ in Appendix C 3.

Considering Eq. (6) with static fields t, V, we can artificially introduce [29] an additional Hilbert space associated to $\Phi = 0, 2\pi, 4\pi$. To manifestly illustrate the effect of phase slips, we define $\omega = e^{i2\pi/3}$ and the following two matrices in the space of groundstate manifold

$$\sigma_\Phi = \begin{pmatrix} 1 & & \\ & \omega & \\ & & \omega^2 \end{pmatrix}, \qquad \tau_\Phi = \begin{pmatrix} 0 & 0 & 1 \\ 1 & 0 & 0 \\ 0 & 1 & 0 \end{pmatrix}. \tag{16}$$

Here, τ_Φ are clock matrices $\sigma_\Phi\tau_\Phi = \omega\tau_\Phi\sigma_\Phi$, $\tau_\Phi^3 = 1$. The phase slips accompanying spinon hoppings, are taken into account by replacement $t \to t\sigma_\Phi$.

The infinite resummation of phase slips of the latter in the partition sum leads to an effective Hamiltonian derived in Appendix D 2

$$\begin{aligned} H_{\text{eff}} = {} & [H_c + \sum_m \lambda(f_{\alpha,m}^\dagger f_{\alpha,m} - Q)]\mathbf{1}_\Phi - \Gamma(\tau_\Phi + \tau_\Phi^{-1}) \\ & + \sum_m \left[V f_{\alpha,m}^\dagger c_{\alpha,m}\mathbf{1}_\Phi - t f_{\alpha,m}^\dagger f_{\alpha,m+1}\sigma_\Phi + H.c.\right]. \end{aligned} \tag{17}$$

In the formulation of Eq. (17), two limiting cases become apparent. First, $\Gamma/t \to 0$ representing the 3CK phase. Second, perturbation about $\Gamma/t\to\infty$ demonstrates that t is RG irrelevant and the LFL is restored.

To study the transition between these two limiting phases, we consider the helical (i.e. Fourier transformed) basis $\tilde{f}_{\alpha,h} = \sum_m e^{-ihm} f_{\alpha,m}/\sqrt{3}$. A phase slip $t\to\omega t$ is equivalent to the instantaneous jump of the spinon energy $(t,-2t,t)\to(t,t,-2t)$ for $h = (-2\pi/3, 0, 2\pi/3)$, Fig. 3 **b**. Due to hybridization with conduction electrons a phase slip triggers an Anderson orthogonality catastrophe and thereby logarithmic attraction of opposite phase slips, $\Delta\tau$ apart, with an effective action

$$S_{\text{slips}} = \kappa \ln|\Delta\tau|. \tag{18}$$

Here

$$\kappa = \frac{2N}{\pi^2}\left[\arctan\left(\frac{3t\Delta}{\Delta^2+\lambda^2}\right)\right]^2 \tag{19}$$

is the stiffness of interaction as determined by the perturbative inclusion of a single pair of opposite phase slips at distance $\Delta\tau$ in the fermionic partition sum, see Appendix D 1. Integration over $\Delta\tau$ leads to the free energy

$$F = \ln(g_N)T + \mathcal{C}(\Gamma^2/\lambda)(T/\lambda)^{\kappa-1}, \tag{20}$$

where we included the effect of the ground state degeneracy g_N, Eq. (5), and $\mathcal{C}$ is a constant. This signals a quantum phase transition when the phase-slips overpower the first term at $\kappa = 2$, corresponding to, Fig. 2 **c**,

$$t_c \sim T_K \sin(\pi q)/\sqrt{N}. \tag{21}$$

The residual entropy at the QCP is enhanced to $S = \ln(g_N) + \mathcal{C}\Gamma^2/\lambda^2 + \mathcal{O}(\Gamma^4/\lambda^4)$ by the instanton contribution, in consistency with the g-theorem [61]. The present model of logarithmically interacting particles on a ring of circumference $1/T$ can be cast into renormalization group language [62]: Γ renormalizes to infinity (zero) for $t<t_c$ ($t_c<t$). However, contrary to the Berezinskii-Kosterlitz-Thouless transition, the stiffness κ does not flow.

So far, the deconfinement transition was studied by first locking Φ into one of the minima of Eq. (9) and subsequent perturbative inclusion of phase slips. The same transition may also be studied in a dual language (approaching the red star of Fig. 1 **b** from the right). In this case Φ is free to fluctuate and $\beta \ll 1$ is considered as a perturbation. From this perspective, the 3CK (FL) is the phase where β is relevant (irrelevant). Crucially, near the transition, the dynamics of the Φ field is overdamped due to the interaction with the conduction bath, see Eq. (12a), (13a) The problem of dissipative tunneling, i.e. $S = S_{\rm diss} - \int d\tau N T_K \beta \cos[\Phi(\tau)]$, for small β yields a scaling equation

$$\frac{d\beta}{d\ell} = \left(1 - \frac{1}{\eta}\right)\beta \tag{22}$$

where $d\ell = -\log D$ in terms of the running cut-off [63, 64], while the non-analytical nature of the "kinetic" (i.e. damping) term is believed to prevent a renormalization of η to all orders [62]. The condition $\eta > 1$ for relevant β is parametrically equivalent to $t > t_c$, with t_c given in Eq. (21). In the dual language it is manifest that Goldstone bosons $\vec{x}$ do not affect the nature or position of the transition because they are by construction perpendicular to Φ.

D. 3CK phase in fractionalized language

Before concluding, we briefly reiterate the connection to the three channel Kondo problem for $T_K \ll J_H$ in fractionalization language:

In this limit it is convenient to evaluate Eq. (17) in a gauge in which t is real and positive. Since Γ is irrelevant in this phase, σ_Φ is conserved. We project on the ground state (zero helicity $h = 0$) of the f-electrons (Fig. 3 **a**) and obtain the effective Kondo Lagrangian

$$\mathcal{L}_{\rm Kondo} = \sum_m \left[(\tilde{f}^\dagger_{\alpha,0} V_m c_{\alpha,m} + c.c.) + \frac{|V_m|^2}{J_K} \right], \tag{23}$$

with constraint $\tilde{f}^\dagger_{\alpha,0}\tilde{f}_{\alpha,0} = 3Q$. As anticipated previously, three channels of conduction electrons are screening a single spin and 3CK physics is expected. The soft modes associated with rotations of $|V_m|$ are gapped for $T_K/J_H > 0$ enforcing $V_m = Ve^{ia_m}$. Based on this observation, we conjecture that the physics discussed here for the 3CK phases of our Kondo triangle applies more generally to single-impurity three-channel Kondo systems and more generic oversceened Kondo problems.

VI. CONCLUSION

We conclude with a discussion of multi-channel Kondo phases as representatives of topological order and of possible experimental and numerical implications of our findings.

A. Signatures of topological order

While there is no magnetic ordering in any of the phases, the symmetric ring exchange operator $\mathcal{O}_s = d_{abc}\hat{S}^a_1\hat{S}^b_2\hat{S}^c_3$ displays order in the 3CK phase. The ordering of such a composite operator is similar to *order by disorder* [65–67] or *vestigial order* [68] phenomena and would suggest a characterization of the 3CK phase in terms of a generalization of spontaneous symmetry breaking.

However, we here propose a different interpretation and put forward the hypothesis that multi-channel Kondo states display a form of topological order which is similar to the quantum order in gapless QSLs. For the 3CK phase scrutinized here, the evidence is as follows:

First, as mentioned the 3CK phase does not break any of the physical symmetries in the original model (1), even when the $\mathcal{O}_s$ orders. This invalidates any interpretation of the 3CK in terms of spontaneous symmetry breaking - instead we have presented a categorization using the projective symmetry group. Second, regarded as an operator in the gauge theory, $\mathcal{O}_s \sim {\rm Re}(e^{i\sum_m A_m})$ is a miniature Wilson loop. In macroscopically extended systems, this would be taken as a clear signal of deconfinement. Third, the order of $\mathcal{O}_s$ is destroyed by the proliferation, or "condensation", of monopoles in the FL, which on the other hand are gapped in the 3CK phase. This is reminiscent of the situation in QED_3, while the expulsion of topological defects is generically a defining characteristic of topological states.[69] Finally, the 3CK displays an irrational ground state degeneracy indicating gapless anyonic excitations, another striking signature of topological order.

At the same time, multichannel Kondo states are often unstable towards anisotropic coupling to the leads (see, e.g. Refs. 70 and 71 for exceptions). As mentioned, while the 3CK phase studied here is stable for unequal J_H it is unstable if J_K are unequal. This suggests the interpretation of the 3CK phase as a symmetry protected topological state of matter or as a deconfined quantum critical fixed point.

B. Relevance for experiment and numerics

Beyond its purpose as an analytically tractable toy model, our investigations are relevant to the simplest cluster-dynamical mean field theory [72, 73] approaches to Hubbard models on triangular lattices which have enjoyed increased interest in recent times [74, 75]. The SU(4) case studied here might be of importance for twisted bilayer graphene [76, 77] with approximate valley symmetry. Emergent SU(4) symmetric spin interactions [78–80] were also recently predicted in spin-orbit coupled transition metal trihalides with low-lying $J_{\rm eff} = 3/2$ quartets [81]. SU(N) symmetric interactions of strongly correlated fermions with large flavor number N have moreover been realized in cold atomic quantum em-

ulators [82, 83]. We conclude with the prospect of directly probing the presented theory in quantum dot experiments: Recent advance on SU(4) impurities [84], triangle [85], and three channel [86] Kondo physics may allow to artificially fabricate the setup Fig. 1 **a** and thereby conduct an experimental study of the deconfinement transition.

ACKNOWLEDGMENTS

The authors appreciate discussions with P. Chandra, W. Metzner, Th. Schäfer and E. Sela. E.J.K. was supported by DOE Basic Energy Sciences grant DE-FG02-99ER45790. P. C. and Y. K. were support by NSF grant DMR-1830707.

Appendix A: Mapping to three channel Kondo problem

This section is devoted to the mapping of the frustrated triangle to a three channel Kondo problem and contains details for Sec. III of the main text. This mapping is possible for the sequence of models with $SU(4), SU(7), SU(10)\ldots$ (i.e. $N \in 3\mathbb{N}+1$) symmetry at filling $q = 1/4, 2/7, 3/10, \ldots$ (i.e. $Q = (N-1)/3$) and is valid when J_H is the largest scale.

1. Solution of the triangle alone

We represent a given spin configuration with fixed particle number per site $Q = (N-1)/3$ by

$$|\alpha_1 \ldots \alpha_Q; \alpha_{Q+1} \ldots \alpha_{2Q}; \alpha_{2Q+1} \ldots \alpha_{3Q}\rangle = f^\dagger_{1,\alpha_1} \ldots f^\dagger_{1,\alpha_Q} f^\dagger_{2,\alpha_{Q+1}} \ldots f^\dagger_{2,\alpha_{2Q}} f^\dagger_{3,\alpha_{2Q+1}} \ldots f^\dagger_{3,\alpha_{3Q}} |\underline{0}\rangle . \tag{A1}$$

In this manifold, the spin is faithfully represented as

$$\hat{S}^a_m = f^\dagger_{\alpha,m} \sigma^a_{\alpha\beta} f_{m,\beta}. \tag{A2}$$

We next act on Eq. (A1) with the Hamiltonian

$$H_H = \frac{J_H}{N} \sum_{m=1}^{3} \Big(f^\dagger_{m,\alpha} f_{m,\beta} f^\dagger_{m+1,\beta} f_{m+1,\alpha} - \frac{f^\dagger_{m,\alpha} f_{m,\alpha} f^\dagger_{m+1,\beta} f_{m+1,\beta}}{N} \Big). \tag{A3}$$

The last term yields a mere shift of energy $3Q^2 J_H/N^2$ for any of the states Eq. (A1), so we omit it. The action of the first term is the sum of permutations of two spin indices from adjacent sites,

$$\begin{aligned} H_H |\alpha_1 \ldots \alpha_Q; \alpha_{Q+1} \ldots \alpha_{2Q}; \alpha_{2Q+1} \ldots \alpha_{(N-1)}\rangle = \frac{J_H}{N} \Big\{ & |\alpha_{Q+1} \ldots \alpha_Q; \alpha_1 \ldots \alpha_{2Q}; \alpha_{2Q+1} \ldots \alpha_{(N-1)}\rangle \\ & + |\alpha_1, \alpha_{Q+1} \ldots \alpha_Q; \alpha_2, \alpha_{Q+2} \ldots \alpha_{2Q}; \alpha_{2Q+1} \ldots \alpha_{(N-1)}\rangle + (\text{similar perm. between sites 1,2}) \\ & + |\alpha_1 \ldots \alpha_Q; \alpha_{2Q+1} \ldots \alpha_{2Q}; \alpha_{Q+1} \ldots \alpha_{(N-1)}\rangle + (\text{similar perm. between sites 2,3}) \\ & + |\alpha_{2Q+1} \ldots \alpha_Q; \alpha_{Q+1} \ldots \alpha_{2Q}; \alpha_1 \ldots \alpha_{(N-1)}\rangle + (\text{similar perm. between sites 3,1}) \Big\}. \end{aligned} \tag{A4}$$

Therefore, eigenstates $|\psi\rangle$ are obtained by sums over symmetric/antisymmetric permutations (Einstein summation convention is employed.)

$$|\psi\rangle = t_{\alpha_1,\ldots,\alpha_Q;\alpha_{Q+1}\ldots\alpha_{2Q};\alpha_{2Q+1}+\alpha_{3Q}} |\alpha_1, \ldots, \alpha_Q, \alpha_{Q+1} \ldots \alpha_{2Q}, \alpha_{2Q+1} + \alpha_{3Q}\rangle . \tag{A5}$$

We concentrate on the ground state, where the tensor has the following antisymmetry properties

$$t_{\alpha_1,\alpha_2\ldots,\alpha_Q;\alpha_{Q+1}\ldots\alpha_{2Q};\alpha_{2Q+1}+\alpha_{3Q}} = -t_{\alpha_2,\alpha_1\ldots,\alpha_Q;\alpha_{Q+1}\ldots\alpha_{2Q};\alpha_{2Q+1}+\alpha_{3Q}} \qquad \text{(Fermi-Dirac statistics within a given site)} \tag{A6}$$

$$t_{\alpha_1,\alpha_2\ldots,\alpha_Q;\alpha_{Q+1}\ldots\alpha_{2Q};\alpha_{2Q+1}+\alpha_{3Q}} = -t_{\alpha_{Q+1},\ldots,\alpha_Q;\alpha_1\ldots\alpha_{2Q};\alpha_{2Q+1}+\alpha_{3Q}} \qquad (H_H \text{ favors pairwise antisymmetry across sites}) \tag{A7}$$

To get the total number of states, we start by overcounting allowed possibilities. There are N options to place α_1, $N-1$ to place α_2 etc., leading to

$$\frac{N!}{(N-3Q)!} \tag{A8}$$

states. However, we overcounted $3Q!$ different permutations, so the actual number of states is just

$$\binom{N}{3Q} = \binom{N}{N-1} = N. \tag{A9}$$

Thus, the following completely antisymmetriezed eigenstates are the ground state of the triangle at filling Q

$$|\alpha_N\rangle = \frac{\epsilon_{\alpha_1\dots\alpha_N}}{\sqrt{\mathcal{N}}}\,|\alpha_1\dots\alpha_Q;\alpha_{Q+1}\dots\alpha_{2Q};\alpha_{2Q+1}\dots\alpha_{(N-1)}\rangle\,. \tag{A10}$$

Here and in the following we label numerical normalization factors by $\mathcal{N}$. This concludes the derivation of Eq. (3). There we use the notation

$$|\text{singlet}, m=1\rangle = \frac{\epsilon_{\alpha_1\dots\alpha_N}}{\sqrt{\mathcal{N}}}\times |\alpha_1\dots\alpha_{Q+1};\alpha_{Q+2}\dots\alpha_{2Q+1};\alpha_{2Q+2}\dots\alpha_N\rangle\,, \tag{A11}$$

and analogously for $m = 2, 3$.

2. Effective low-energy Hamiltonian

As a next step, we project the Kondo-triangle Hamiltonian onto the groundstate manifold spanned by the N states Eq. (A10). We begin by determining the spin-representation within the manifold of states Eq. (A10)

$$\begin{aligned}\langle\alpha_N|\hat{S}^a_m|\alpha'_N\rangle =& \frac{\sigma^a_{\beta\beta'}\epsilon_{\alpha_1\dots\alpha_N}\epsilon_{\alpha'_1\dots\alpha'_N}}{\mathcal{N}} \\ & \langle\alpha_1\dots\alpha_Q;\alpha_{Q+1}\dots\alpha_{2Q};\alpha_{2Q+1}\dots\alpha_{N-1}|\ \underbrace{f^\dagger_{m,\beta}f_{m,\beta'}}_{\delta_{\beta\beta'}-f_{m,\beta'}f^\dagger_{m,\beta}}\ |\alpha'_1\dots\alpha_{Q'};\alpha'_{Q+1}\dots\alpha'_{2Q};\alpha'_{2Q+1}\dots\alpha'_{(N-1)}\rangle \\ =& -\tilde{\mathcal{N}}\sigma^a_{\alpha'_N\alpha_N}\,.\end{aligned} \tag{A12}$$

This result immediately follows from the consideration that all spin quantum numbers except $\alpha_N(\alpha'_N)$ have been used in the ket (bra). Thus the index of the creation operator $\beta = \alpha'_N$ ($\beta' = \alpha_N$) unless $\beta = \beta'$. We further used $\mathrm{tr}[\sigma^a] = 0$. Instead of explicitly calculating the positive proportionality constant we show that $\tilde{\mathcal{N}} = 1$ by

$$\begin{aligned}\sum_{N,N'}|\langle\alpha_N|\hat{S}^a_m|\alpha'_N\rangle|^2 &= \mathrm{tr}[[\sigma^a]^2] \\ &= \tilde{\mathcal{N}}^2\mathrm{tr}[\{[\sigma^a]^T\}^2].\end{aligned} \tag{A13}$$

Here, the first equality follows from the completeness of $\{|\alpha_N\rangle\}$ and the second equality from the evaluation of the matrix element. Therefore, the effective Hamiltonian has the form

$$H_{\text{eff}} = H_c - \frac{J_K}{N}\sum_{m=1}^{3}[\hat{S}^a]^T c^\dagger_m\sigma^a c_m. \tag{A14}$$

As a final step, we reverse particle and hole operators $c_m \to h^\dagger_m, c^\dagger_m \to h_m$, then

$$H_{\text{eff}} = H_c + \frac{J_K}{N}\sum_{m=1}^{3}[\hat{S}^a]^T h^\dagger_m[\sigma^a]^T h_m. \tag{A15}$$

This is the origin of Eq. (4) in the main text. To see that Eq. (4), in which spin operators are transposed, is equivalent to the standard three channel Kondo model

$$H_{3\text{CK}} = H_c + \frac{J_K}{N}\sum_{m=1}^{3}\hat{S}^a h^\dagger_m\sigma^a h_m, \tag{A16}$$

it is sufficient to realize that the SU(N)-invariant interaction can be reexpressed using the Fierz identity

$$[\sigma^a]_{\alpha\beta}[\sigma^a]_{\gamma\delta} = \delta_{\alpha\delta}\delta_{\beta\gamma} - \frac{1}{N}\delta_{\alpha\beta}\delta_{\gamma\delta}, \tag{A17}$$

which is invariant under simultaneous transposition operation $(\alpha,\gamma)\leftrightarrow(\beta,\delta)$.

3. Robustness against inhomogeneity

At strong coupling the triangle is robust against moderate inhomogeneities in J_H, as can be seen by the following evaluation of matrix elements of $\delta H = \delta J_H\hat{S}^a_1\hat{S}^a_2$

$$\begin{aligned}\langle\alpha_N|\delta H|\alpha'_N\rangle &= \delta J_H\sum_{\tilde{\alpha}_N}\langle\alpha_N|\hat{S}^a_1|\tilde{\alpha}_N\rangle\langle\tilde{\alpha}_N|\hat{S}^a_2|\alpha'_N\rangle \\ &= \tilde{\mathcal{N}}^2\sum_a\sum_{\tilde{\alpha}_N}[\sigma^a]_{\alpha'_N\tilde{\alpha}_N}[\sigma^a]_{\tilde{\alpha}_N\alpha_N} \propto \delta_{\alpha'_N\alpha_N}.\end{aligned} \tag{A18}$$

Thus, inhomogeneities projected to the ground state manifold are proportional to the unit matrix and do not lift the degeneracy of states $|\alpha_N\rangle$.

Appendix B: Impurity partition sum, static evaluation

In this section we present technical details on the evaluation of the partition sum. Throughout the paper, we

consider the partition sum (and thus free energy and effective action) of the impurity alone. This is defined as $\mathcal{Z}_{\text{impurity}} = \mathcal{Z}_{\text{total}}/\mathcal{Z}_{\text{no impurity}}$, where Z_{total} is given by

$$\mathcal{Z}_{\text{total}} = \prod_{m=1}^{3} \int_0^\infty \mathcal{D}V_m V_m \int_{-i\infty}^{i\infty} \mathcal{D}\lambda_m \int_{\mathbb{C}^2} \mathcal{D}[t_m, t_m^*] \int \mathcal{D}[c_m, f_m] e^{-S[V_m,\lambda_m,t_m,c_m,f_m]}, \tag{B1}$$

Note that we employ Read-Newns gauge ($V_m > 0$) throughout this section. The partition sum $\mathcal{Z}_{\text{no impurity}}$ is the same partition sum of the three wires but without any Kondo impurities.

1. Diagonalization of spinon Hamiltonian

The spinon Hamiltonian, see also Eq. (6) of the main text, has the form

$$H_t = -t f^\dagger \begin{pmatrix} 0 & e^{iA_1} & e^{-iA_3} \\ e^{-iA_1} & 0 & e^{iA_2} \\ e^{iA_3} & e^{-iA_2} & 0 \end{pmatrix} f, \tag{B2}$$

where we use the three component notation $f = (f_1, f_2, f_3)$, and similarly for $c(\boldsymbol{x}) = (c_1(\boldsymbol{x}), c_2(\boldsymbol{x}), c_3(\boldsymbol{x}))$ on each site of the wires. We rotate $f = U\tilde{f}$ and $c = U\tilde{c}$ electrons by $U = \text{diag}(e^{i(A_1-\Phi/3)}, 1, e^{-i(A_2-\Phi/3)})$, leading to

$$H_t = -t \tilde{f}^\dagger \begin{pmatrix} 0 & e^{i\Phi/3} & e^{-i\Phi/3} \\ e^{-i\Phi/3} & 0 & e^{i\Phi/3} \\ e^{i\Phi/3} & e^{-i\Phi/3} & 0 \end{pmatrix} \tilde{f}. \tag{B3}$$

This rotation appears at the expense of a vector potential

$$(c^\dagger, f^\dagger)\partial_\tau (c, f)^T = (\tilde{c}^\dagger, \tilde{f}^\dagger)[\partial_\tau + i\mathcal{A}](\tilde{c}, \tilde{f})^T, \tag{B4}$$

where

$$\mathcal{A} = -iU^\dagger \partial_\tau U = \text{diag}(\dot{A}_1 - \dot{\Phi}/3, 0, -[\dot{A}_2 - \dot{\Phi}/3]). \tag{B5}$$

It is furthermore useful to expand $\tilde{f}, \tilde{c}$ in eigenstates with instantaneous energy $\epsilon_k = -2t\cos(k + \Phi(\tau)/3)$

$$|\psi_k\rangle = \frac{1}{\sqrt{3}} \begin{pmatrix} e^{-ik} \\ 1 \\ e^{ik} \end{pmatrix}, \quad k = 0, \pm\frac{2\pi}{3}. \tag{B6}$$

In this basis the Berry connection is $\mathcal{A}_{k'k} = ([\dot{A}_1 - \dot{\Phi}/3]e^{i(k'-k)} - [\dot{A}_2 - \dot{\Phi}/3]e^{-i(k'-k)})/3$. In summary, the total Lagrangian under consideration is (we employ the notation $D_\tau = \partial_\tau + i\mathcal{A}$ and $\lambda_k = \lambda + \epsilon_k(\Phi)$)

$$\mathcal{L} = \sum_{k,k'} \begin{pmatrix} \cdots & c^\dagger_{\alpha,k}(\boldsymbol{p}) & \cdots & f^\dagger_{\alpha,k} \end{pmatrix} \left(\begin{array}{c|c} [D_\tau]_{k,k'} + \epsilon(\boldsymbol{p})\delta_{\boldsymbol{p},\boldsymbol{p}'}\delta_{kk'} & V\delta_{kk'} \\ \hline V\delta_{kk'} & [D_\tau]_{k,k'} + \lambda_k\delta_{kk'} \end{array}\right) \begin{pmatrix} \vdots \\ c_{\alpha,k'}(\boldsymbol{p}') \\ \vdots \\ f_{\alpha,k'} \end{pmatrix}$$
$$+3\left(N\frac{t^2}{J_K} + N\frac{V^2}{J_K} - \lambda q N\right). \tag{B7}$$

2. Static fields and mean field solution

We begin by studying the mean field solution. At this level, we consider all bosonic fields $V > 0, t > 0, \Phi = \sum_m A_m$ as constant variational parameters, and $\mathcal{A} = 0$. The fermionic integral yields Eq. (7). The mean field equations involve the following two integrals

$$n_F \equiv I_1(\lambda/\Delta) = T\sum_n \frac{e^{i\epsilon_n\eta}}{i\epsilon_n - \lambda + i\Delta s(\epsilon_n/D)}$$
$$\simeq \text{arccot}(\lambda/\Delta)/\pi =: \delta(\lambda/\Delta)/\pi, \tag{B8a}$$
$$I_2(\lambda + i\Delta) = T\sum_n \frac{is(\epsilon_n/D)e^{i\epsilon_n\eta}}{i\epsilon_n - \lambda + i\Delta s(\epsilon_n/D)}$$
$$\simeq -\frac{\ln(|\lambda + i\Delta|\eta) + \gamma_{\text{EM}}}{\pi}. \tag{B8b}$$

Here, γ_{EM} is the Euler Mascheroni constant (with our regularization scheme $T_K = e^{-1/[\rho J_K]-\gamma_{\text{EM}}}/\eta$) and $\simeq$ im-

plies a zero temperature calculation. Note that δ becomes a step function (from π down to 0) as $\Delta \to 0$.

Having established these prerequisites, we are now in the position of imposing the mean field equations

$$\frac{1}{N}\frac{\partial F}{\partial \lambda} = \sum_k \left(I_1\left(\frac{\lambda_k}{\Delta}\right) - q \right) \stackrel{!}{=} 0, \tag{B9a}$$

$$\frac{1}{N}\frac{\partial F}{\partial \Delta} = \sum_k \left(-I_2\left(\frac{\lambda_k}{\Delta}\right) + \frac{1}{\pi \rho J_K} \right) \stackrel{!}{=} 0, \tag{B9b}$$

$$\frac{1}{N}\frac{\partial F}{\partial t} = \sum_k \left(\frac{\partial \epsilon_k}{\partial t} I_1\left(\frac{\lambda_k}{\Delta}\right) + \frac{2t}{J_H} \right) \stackrel{!}{=} 0, \tag{B9c}$$

$$\frac{1}{N}\frac{\partial F}{\partial \Phi} = \sum_k \frac{\partial \epsilon_k}{\partial \Phi} I_1\left(\frac{\lambda_k}{\Delta}\right) \stackrel{!}{=} 0. \tag{B9d}$$

We readily see that ground state solutions are given by $\Phi \in 2\pi\mathbb{Z}$. Then the first three equations yield cf. Eqs. (8),

$$3\pi q = \sum_k \delta_k = \delta_0 + 2\delta_{2\pi/3} \tag{B10a}$$

$$T_K^3 = \prod_k \sqrt{\lambda_k^2 + \Delta^2} = \frac{\Delta^3}{\sin(\delta_3)\sin(\delta_{2\pi/3})^2} \tag{B10b}$$

$$2(\delta_0 - \delta_{2\pi/3}) = 3\frac{2\pi t}{J_H} = \frac{2\pi}{J_H}(\lambda_{2\pi/3} - \lambda_0) = \frac{2\pi\Delta}{J_H}(\cot(\delta_{2\pi/3}) - \cot(\delta_0)) = 2\sin(\delta_0 - \delta_{2\pi/3})\frac{\pi T_K}{J_H}\sqrt[3]{\frac{1}{\sin(\delta_{2\pi/3})\sin^2(\delta_0)}} \tag{B10c}$$

We readily recognize the Kondo solution $t = 0$, $\delta_k = \pi q, \Delta = T_K \sin(\pi q)$, which is present for any T_K/J_H. The last equation is the origin of Eq. (8c).

3. Finite temperatures

Of the presented finite temperature phases in Fig. 1 **b** of the main text, the presence of the LFL and local moment phase is obvious. The existence of an LFL* and of the 3CK phase is discussed now by showing that there is a mean field transition $T_{\mathrm{SL}} = J_H q(1-q)$ below which t develops a vacuum expectation value and a lower transition T_K^{eff} at which V spontaneously develops. For the perturbative solution in Δ at finite T we use

$$n_f(\lambda) = I_1 = n_{\mathrm{FD}}(\lambda) = \frac{1 - \tanh(\lambda/2T)}{2} \tag{B11}$$

and, perturbatively in Δ,

$$I_2(\lambda) = T\sum_{\epsilon_n > 0}\left(\frac{i}{i\epsilon_n - \lambda} + \frac{i}{i\epsilon_n + \lambda}\right) \simeq \frac{\ln(D/T)}{\pi} - \frac{\psi^{(0)}\left(\frac{i\lambda/T+\pi}{2\pi}\right) + \psi^{(0)}\left(\frac{\pi - i\lambda/T}{2\pi}\right)}{2\pi} \tag{B12}$$

The mean field equations (perturbative in Δ) are then

$$n_{\mathrm{FD}}(\lambda - 2t) = q + \frac{2t}{J_H} = q + \frac{\lambda}{J_H} - \frac{\lambda - 2t}{J_H}, \tag{B13}$$

$$n_{\mathrm{FD}}(\lambda + t) = q - \frac{t}{J_H}, \tag{B14}$$

$$3\ln\left(\frac{T_K}{T}\right) = \sum_k \left(\frac{\psi^{(0)}\left(\frac{i\lambda_k/T+\pi}{2\pi}\right) + \psi^{(0)}\left(\frac{\pi - i\lambda_k/T}{2\pi}\right)}{2} - \frac{\psi^{(0)}\left(\frac{i\lambda_{t=0}/T+\pi}{2\pi}\right) + \psi^{(0)}\left(\frac{\pi - i\lambda_{t=0}/T}{2\pi.}\right)}{2} \right), \tag{B15}$$

with $\lambda_k = (\lambda + t, \lambda + t, \lambda - 2t)$ and $\lambda_{t=0} = 2T\mathrm{artanh}(1 - 2q)$ the solution without t. The mean field spin-liquid transition temperature is obtained by expanding the first

two equations in t

$$q = n_{\rm FD}(\lambda) \Leftrightarrow \lambda = 2T\,\mathrm{artanh}\,(1-2q)\,, \tag{B16}$$

$$\frac{1}{J_H} = -\frac{\partial n_{\rm FD}}{\partial \lambda} = \frac{1}{4T\cosh^2(\lambda/2T)} = \frac{1}{4T\cosh^2(\mathrm{artanh}(1-2q))}. \tag{B17}$$

Thus for $0 < q < 1/3$

$$\frac{T_{\rm SL}}{J_H} = \frac{1}{4\pi\cosh^2(\mathrm{artanh}(1-2q))} = q(1-q). \tag{B18}$$

For the solution of $T_K^{\rm eff} < T_{\rm SL}$ it is more convenient to use

$$n_k = n_{\rm FD}(\lambda_k) \tag{B19}$$

and insert this into

$$3q = 2n_{2\pi/3} + n_0, \tag{B20}$$

$$\Delta n \equiv n_0 - n_{2\pi/3} = \frac{3t}{J_H} = \frac{T}{J_H}(\bar\lambda_{2\pi/3} - \bar\lambda_0). \tag{B21}$$

We use

$$\bar\lambda_{t=0} = \lambda_{t=0}/T = 2\mathrm{artanh}(1-2q), \tag{B22}$$

$$\bar\lambda_{2\pi/3} = \lambda_{2\pi/3}/T = 2\mathrm{artanh}(1-2n_{2\pi/3}) = 2\mathrm{artanh}(1-2q+\frac{2\Delta n}{3}), \tag{B23}$$

$$\bar\lambda_0 = \lambda_0/T = 2\mathrm{artanh}(1-2n_0) = 2\mathrm{artanh}(1-2q-\frac{4\Delta n}{3}). \tag{B24}$$

to replace temperature in Eq. (B15)

$$T = T_K \prod_k \left[\exp\left(\frac{\psi^{(0)}\left(\frac{i\lambda_k/T+\pi}{2\pi}\right)+\psi^{(0)}\left(\frac{\pi-i\lambda_k/T}{2\pi}\right)}{2} - \frac{\psi^{(0)}\left(\frac{i\lambda_{t=0}/T+\pi}{2\pi}\right)+\psi^{(0)}\left(\frac{\pi-i\lambda_{t=0}/T}{2\pi}\right)}{2}\right)\right]^{-1/3}$$
$$\equiv T_K \underbrace{g(\lambda_{t=0}, \lambda_{2\pi/3}(\Delta n), \lambda_0(\Delta n))}_{:=f(\Delta n)}. \tag{B25}$$

We thus reduced the finite temperature Kondo transition in the presence of finite t, i.e. finite Δn to a single equation for Δn

$$\Delta n = \frac{T_K}{J_H} f(\Delta n)[\bar\lambda_{2\pi/3} - \bar\lambda_0]. \tag{B26}$$

Numerical solution of this equation demonstrates the existence of $0 < T_K^{\rm eff} < T_{\rm SL}$ for sufficiently small T_K/J_H.

4. Landau Free energy (perturbative in t)

We consider the case of small t and employ $\xi = \lambda + i\Delta = T_K e^{i\pi q}$ [87]

$$V[\Phi] = \frac{N}{\pi}\sum_k \mathrm{Im}\left[(\lambda_k + i\Delta)\ln\left(\frac{(\lambda_k+i\Delta)}{eT_K e^{i\pi q}}\right)\right] \tag{B27}$$

$$= \frac{N}{\pi}\sum_k \mathrm{Im}\left[\sum_k \frac{\epsilon_k^2}{2\xi} - \frac{\epsilon_k^3}{6\xi^2} + \frac{\epsilon_k^4}{12\xi^3}\right]$$

$$= \frac{T_K N}{\pi}\Big[-3\bar t^2\sin(\pi q) - \cos(\Phi)\bar t^3\sin(2\pi q) - 3\bar t^4\sin(3\pi q)/2\Big]. \tag{B28}$$

Up to the effect of biquadratic and ring exchange terms (see following section), as well as the Hubbard-Stratonovich term $3t^2/J_H$, this expression yields Eq. (9) of the main text.

5. Ring exchange and biquadratic terms

In the large N limit, the transition between LFL and 3CK appears to be first order. Here, we consider additional terms which ultimately overcome the first order behavior. We need

$$\langle f_m f_{m+1}^\dagger\rangle \simeq -\int (d\epsilon)\frac{t_m}{[i\epsilon+\lambda+i\Delta\mathrm{sign}(\epsilon)]^2} = \frac{t_m}{\pi T_K}\sin(\pi q) \tag{B29}$$

We first study ring-exchange terms of the form

$$H_3 = -\pi^2\frac{J_s}{N}d_{abc}\hat S_1^a\hat S_2^b\hat S_3^c - \pi^2\frac{J_\chi}{N}f_{abc}\hat S_1^a\hat S_2^b\hat S_3^c. \tag{B30}$$

These terms can be evaluated on mean field level as

($T_{abc} = J_s d_{abc} + J_\chi f_{abc}$ and we use $t_m = te^{i\Phi/3}$.)

$$\begin{aligned} H_3 &\simeq -\pi^2 \frac{T_{abc}}{N} \langle f_1^\dagger \sigma^a f_1 f_2^\dagger \sigma^b f_2 f_3^\dagger \sigma^c f_3 \rangle \\ &= \frac{T_{abc}(\sin \pi q)^3}{\pi T_K^3 N} [t_1 t_2 t_3 \mathrm{tr}(\sigma^a \sigma^b \sigma^c) + \bar{t}_3 \bar{t}_2 \bar{t}_1 \mathrm{tr}(\sigma^a \sigma^c \sigma^b)] \\ &= J_s (\sin \pi q)^3 \frac{d_{abc}}{\pi T_K^3 N} \underbrace{\mathrm{tr}(\sigma^a \{\sigma^b, \sigma^c\})}_{d_{abc}} t^3 \cos(\Phi) \\ &+ J_\chi (\sin \pi q)^3 \frac{i f_{abc}}{\pi T_K^3 N} \underbrace{\mathrm{tr}(\sigma^a [\sigma^b, \sigma^c])}_{i f_{abc}} t^3 \sin(\Phi) \\ &= N \frac{J_s (\sin \pi q)^3}{\pi T_K^3} t^3 \cos(\Phi) + N \frac{J_\chi (\sin \pi q)^3}{\pi T_K^3} t^3 \sin(\Phi) \end{aligned} \tag{B31}$$

We used

$$d_{abc} d_{abc} = N^2 - 4, \; f_{abc} f_{abc} = N^2. \tag{B32}$$

This term enters β in Eq. (9) of the main text.

We furthermore introduce biquadratic interactions

$$H_4 = -\frac{\pi^3 J_4}{2N^3} \sum_m [\hat{S}^a_m \hat{S}^a_{m+1}]^2. \tag{B33}$$

Their mean field decoupling leads to

$$\begin{aligned} H_4 &= -\frac{\pi^3 J_4}{2N^3} \langle\!\langle \sum_m f_m^\dagger \sigma^a f_m f_{m+1}^\dagger \sigma^a f_{m+1} f_m^\dagger \sigma^b f_m f_{m+1}^\dagger \sigma^b f_{m+1} \rangle\!\rangle \\ &= 3t^4 \frac{J_4 \sin(\pi q)^4}{2N^3 \pi T_K^4} \left(\underbrace{\mathrm{tr}[\sigma^a \{\sigma^a, \sigma^b\} \sigma^b]}_{d_{abc} d_{abc}/2} + \underbrace{\mathrm{tr}[\sigma^a \sigma^a]^2}_{=(N^2-1)^2} \right) \\ &\simeq N \frac{3 J_4 \sin(\pi q)^4}{2\pi T_K^4} t^4. \end{aligned} \tag{B34}$$

This term enters γ in Eq. (9) of the main text.

For the plot of Fig. 2 **c** we used $J_{\mathrm{Ring}}^{\mathrm{eff}} = 0.3$ and $J_4^{\mathrm{eff}} = 0.1$ in the effective replacement $J_H \to J_H(1 + d J_{\mathrm{ring}}^{\mathrm{eff}} - d^2 J_4^{\mathrm{eff}})$ in the numerator of Eq. (8c), left.

The replacement is related to the microscopic Hamiltonian as follows. From the mean field evaluation

$$\langle f_m f_{m+1}^\dagger \rangle = \sum_k G_k(0)/3/3 = -d/3\pi. \tag{B35}$$

Therefore, on Hartree-Fock level

$$H_3 \to -N J_s (d/3)^3/\pi = N\pi^2 J_s (t/J_H)^3, \tag{B36}$$

$$H_4 \to N J_4 3 (d/3)^4/(2\pi) = N J_4 3\pi^3 (t/J_H)^4/2 \tag{B37}$$

For small t/J_H this can be reinterpreted as a renormalization

$$\begin{aligned} \frac{t^2}{J_H} &\to \frac{t^2}{J_H(1 - \pi^2 J_s t/J_H^2 - 3\pi^2 (t^2/J_H^3) J_4/2)} \\ &= \frac{t^2}{J_H(1 + \pi J_s/J_H\, d/3 - J_4/J_H\, d^2/3)}. \end{aligned} \tag{B38}$$

Hence we identify

$$J_{\mathrm{Ring}}^{\mathrm{eff}} = \frac{\pi J_s}{3 J_H}, \; J_4^{\mathrm{eff}} = \frac{J_4}{3 J_H}. \tag{B39}$$

Appendix C: Dynamics of Goldstone modes and total flux

In this section we derive the kinetic terms for Goldstone bosons and $\Phi(\tau)$, Eq. (12) of the main text.

1. Goldstone bosons

Before turning to the effective action of Goldstone bosons we comment on the structure

$$\frac{G}{H} = \frac{U(1) \times U(1) \times U(1)}{U(1) \times \mathbb{Z}_3} \tag{C1}$$

of the Goldstone manifold. Smooth transformations of the large group G are represented by three phases χ_m

$$f_m \to U_{mm'} f_{m'}; \quad c_m \to U_{mm'} c_{m'} \quad (U_{mm'} = \delta_{mm'} e^{i\chi_m}) \tag{C2}$$

and per definition $\chi_m(\tau = 1/T) = \chi_m(\tau = 0) + 2\pi j$. Following Sec. II of this supplement, a convenient form of $U = \mathrm{diag}(e^{iA_1 - \Phi/3}, 1, e^{-iA_2 + \Phi/3})$, as it cancels the fluctuating gauge fields on the links. To make the quotient group G/H apparent we factorize

$$U = e^{i\phi} V, \text{ with } \det V = 1. \tag{C3}$$

The naive derivation of the Goldstone action implies the absorption the V (i.e. the $SU(3)$ part of G) into f, c at the expense of a Berry curvature term $\mathcal{A} = -iV^\dagger \partial_\tau V$. The integration of fermions then leads to an effective action in terms of $\mathcal{A}$, an thus implicitly in terms of $A_{1,2,3}$.

However, a certain care is needed for this procedure. The quotient group introduces an emergent $\mathbb{Z}_3$ redundancy which is manifested in non-contractable loops ($j = 0, 1, 2$)

$$e^{i\phi(1/T)} = \omega^j e^{i\phi(0)}, \tag{C4}$$

$$V(1/T) = \bar{\omega}^j V(0). \tag{C5}$$

In particular, the absorption of $f(\tau) = V(\tau)\tilde{f}(\tau)$ changes the boundary conditions ($\tilde{f}(1/T) = -\omega^j f(0)$), i.e. $\tilde{f}(\tau)$ is generically not a fermionic field. We conjecture that the topological nature of $\pi_1(G/H) = \mathbb{Z}_3$ is at the root of the ground state degeneracy of the 3CK phase.

To remedy this problem we choose a parametrization of $U(\tau)$ such that the topological winding is manifest, i.e.

$$\begin{aligned} U(\tau) &= e^{i\bar{\phi}(\tau) + 2\pi i \tau T/3} \\ &\times \begin{pmatrix} e^{-2\pi i \tau T/3} & 0 & 0 \\ 0 & e^{-2\pi i \tau T/3} & 0 \\ 0 & 0 & e^{4\pi i \tau T/3} \end{pmatrix} \bar{V}(\tau), \end{aligned} \tag{C6}$$

where both $e^{i\bar{\phi}(\tau)}$ and $\bar{V}(\tau)$ are periodic in imaginary time. In this parametrization it is apparent that the three different $\mathbb{Z}_3$ sector correspond to the 2π winding

of one of the χ_m. In order to derive the effective action of $V(\tau)$ fluctuations even for non-zero j, we thus absorb $e^{-i\bar{\phi}(\tau)}U(\tau)$ into fermionic fields (without changing their statistics) and integrate fermions subsequently. (with $G_{cf}, G_{cf,k}$ the full Green's function of c and f space and $G_c, G_{c,k}$ the Green's function of conduction electrons and G, G_k the Green's function of f electrons)

$$\begin{aligned} S[A_{2,3}]/N &= -\mathrm{Tr}\ln[-G_{cf}^{-1} + i\mathcal{A}] + \mathrm{tr}\ln[-G_c^{-1} + i\mathcal{A}] \quad \text{(C7)} \\ &\simeq i\mathrm{Tr}[G_{cf}\mathcal{A}] - i\mathrm{tr}[G_c\mathcal{A}] \\ &\quad -\frac{1}{2}\mathrm{Tr}[(G_{cf}\mathcal{A})^2] + \frac{1}{2}\mathrm{tr}[(G_c\mathcal{A})^2]. \quad \text{(C8)} \end{aligned}$$

The symbol "tr" denotes a trace in the space of the three sites and in time, "Tr" additionally includes the 2×2 space of c and f electrons. Specifically, we employ a gauge in which

$$\mathcal{A}_{k'k} = \frac{2\pi jT}{3} + \underbrace{\frac{(\dot{A}_2 - \dot{A}_1)\delta_{kk'} + \left(\dot{A}_1 e^{i(k'-k)} - \dot{A}_2 e^{-i(k'-k)}\right)}{3}}_{=:\bar{\mathcal{A}}_{k'k}}. \quad \text{(C9)}$$

The leading term is fixed by the constraint $\sum_k \delta_k = 3\pi q$ (this result is true beyond mean field)

$$\begin{aligned} S^{(1)} &= i\int d\tau \sum_k G_k(\tau,\tau^+)\mathcal{A}_{kk}(\tau) \\ &= iQ\int d\tau \sum_k \mathcal{A}_{kk}(\tau) \\ &= iQ2\pi m. \quad \text{(C10)} \end{aligned}$$

Note that, since $Q \in \mathbb{Z}$, this expression is invariant yields a trivial phase 2π and can be omitted.

Next we switch to the term of second order in gradients, which can be expressed as

$$S^{(2)} = -\frac{N}{2}\int d\tau \sum_{kk'} I_{kk'}|\mathcal{A}_{kk'}|^2. \quad \text{(C11)}$$

The polarization operator under consideration is

$$\begin{aligned} I_{kk'} &= \int \frac{d\epsilon}{2\pi}\mathrm{tr}^{\mathrm{cf}}[G_{cf,k}(\epsilon)G_{cf,k'}(\epsilon)] - G_{c,k}(\epsilon)G_{c,k'}(\epsilon) \\ &= (1+2(\pi\rho V)^2)\int \frac{d\epsilon}{2\pi} G_k(\epsilon)G_{k'}(\epsilon) \\ &= -\frac{1+2\rho\Delta}{J_H}\begin{pmatrix} \frac{J_H\sin(\delta_+)^2}{\Delta\pi} & \frac{J_H\sin(\delta_+)^2}{\Delta\pi} & 1 \\ \frac{J_H\sin(\delta_+)^2}{\Delta\pi} & \frac{J_H\sin(\delta_+)^2}{\Delta\pi} & 1 \\ 1 & 1 & \frac{J_H\sin(\delta_0)^2}{\Delta\pi} \end{pmatrix}_{kk'}. \quad \text{(C12)} \end{aligned}$$

We here used the short hand notation $\delta_+ = \delta_{2\pi/3}$ and that

$$\int \frac{d\epsilon}{2\pi} G_k(\epsilon)G_{k'}(\epsilon) = -\frac{1}{\pi}\begin{cases} \frac{\Delta}{\Delta^2+\lambda_k^2}, & \lambda_k = \lambda_{k'} \\ \frac{\pi+\arctan(\Delta/\lambda_k)-\arctan(\Delta/\lambda_{k'})}{\lambda_{k'}-\lambda_k}, & \lambda_k<0, \lambda_{k'}>0, \end{cases} \quad \text{(C13)}$$

as well as the mean field equations, Eq. (B10). It is important to realize that remnant $U(1)$ terms and $SU(3)$ terms in Eq. (C11) decouple

$$S^{(2)} = -\frac{N}{2}\int d\tau \sum_{kk'}[I_{kk'}|\bar{\mathcal{A}}_{kk'}|^2 + I_{kk}\left(\frac{2\pi mT}{3}\right)^2\delta_{kk'}]. \quad \text{(C14)}$$

The second term yields a vanishing contribution to the weight in the limit $T\to 0$ and is disregarded. We further use that

$$|\bar{\mathcal{A}}_{kk'}|^2 = \frac{\sum_m \dot{A}_m^2}{18}. \quad \text{(C15)}$$

Here, we have used a gauge transformation to return to generic gauge. The combination of Eq. (C12), (C14), (C15), results in the final result, Eq. (12b) in the main text. To obtain Eq. (15), we employ the parametrization in terms of unit vectors $\hat{e}_m$ and $\sum_m \hat{e}_m\hat{e}_m^T = \mathbf{31}$.

2. Total flux

To obtain the dynamics of the total flux $\Phi(\tau)$ we use the notation $\delta\lambda_k = -2t\left[\cos(k+\Phi/3) - \cos(k)\right]$ and expand the fermionic determinant to second order in $\delta\lambda_k$.

$$
\begin{aligned}
S^{(2)}_{\rm eff} &\simeq \frac{N}{2}\sum_{\omega_m,k}\delta\lambda_k(\omega_m)\delta\lambda_k(-\omega_m)\sum_{\epsilon_n}G_k(\epsilon_n)G_k(\epsilon_n+\omega_m)\\
&\overset{T\to 0}{\simeq} \frac{N\Delta}{2\pi T}\sum_{\omega_m,k}\delta\lambda_k(\omega_m)\delta\lambda_k(-\omega_m)\frac{\ln\left(\frac{\lambda_k^2+\Delta^2}{\lambda_k^2+(\Delta+|\omega|)^2}\right)}{|\omega|(2\Delta+|\omega|)}\\
&= \frac{N\Delta}{2\pi T}\sum_{\omega_m,k}\delta\lambda_k(\omega_m)\delta\lambda_k(-\omega_m)\begin{cases}\left[-\frac{1}{\Delta^2+\lambda_k^2}+|\omega|\frac{\Delta}{(\Delta^2+\lambda_k^2)^2}\right], & |\omega|\ll\lambda_k^2+\Delta^2,\\ -\frac{\ln\left(\frac{\omega^2}{\lambda_k^2+\Delta^2}\right)}{\omega^2}, & |\omega|\gg\lambda_k^2+\Delta^2.\end{cases}
\end{aligned}
\tag{C16}
$$

The equation substantially simplifies for small $t\ll\lambda$, and leads to the kinetic energy of Φ fluctuations

$$
\begin{aligned}
S_{\rm kin}[\Phi] &= N\frac{3t^2T_K\sin(\pi q)}{4\pi T}\sum_{\omega_m}\Phi(\omega_m)\Phi(-\omega_m)\\
&\times\begin{cases}|\omega|\frac{\sin(\pi q)}{T_K^3}, & |\omega|\ll T_K^2,\\ \left[\frac{1}{T_K^2}-\frac{\ln\left(\frac{\omega^2}{T_K^2}\right)}{\omega^2}\right], & |\omega|\gg T_K^2.\end{cases}
\end{aligned}
\tag{C17}
$$

The $|\omega|$ term in the first line is the origin of the damped kinetic term presented in the main text and leads to logarithmic correlators.

3. Estimate of tunneling time and tunneling action.

As demonstrated in the main text, details of the tunneling rate Γ are irrelevant for the transition. We therefore constrain ourselves to merely estimate Γ, based on a tunneling event

$$
\begin{aligned}
\Phi(\tau) &= \frac{\pi}{2}+2\pi\tau/\tau_0\theta(\tau_0^2-4\tau^2)\\
\Rightarrow |\Phi(\omega)|^2 &= \frac{\left(\omega\tau_0\cos\left(\frac{\omega\tau_0}{2}\right)-2\sin\left(\frac{\omega\tau_0}{2}\right)\right)^2}{[\omega\tau_0]^4}.
\end{aligned}
\tag{C18}
$$

In terms of dimensionless parameters $\bar t = t/T_K$ and $\bar\tau_0 = \tau_0/T_K, \bar\omega=\omega\tau_0, \Phi(\omega)=\bar\Phi(\omega\tau_0)$ we obtain

$$
\begin{aligned}
S_{\rm tun}(\bar\tau_0)/N &\sim \beta\bar\tau_0+\bar t^2\sin(\pi q)\bar\tau_0\int_0^\infty|\bar\Phi(\bar\omega)|^2\left(1-\frac{\ln([\sin(\pi q)+\bar\omega]^2\bar\tau_0^2)}{\bar\omega^2\bar\tau_0^2}\right)\\
&\approx \beta\bar\tau_0\left\{1+\frac{\bar t^2\sin(\pi q)}{\beta}\left[\frac{\pi}{6}-\frac{1}{\bar\tau_0^2}\left(\frac{\pi\ln[\sin(\pi q)^2\bar\tau_0^2]}{60}+0.7\right)\right]\right\}.
\end{aligned}
\tag{C19}
$$

To obtain the optimal tunneling time we use that $\bar t\sim\beta/\gamma$ at the mean field first order transition. We thus obtain for any q such that $\sin(\pi q)\sim 1$

$$
\tau_0^{\rm optimal}\sim\frac{1}{T_K}\begin{cases}1, & \gamma\ll 1,\\ \sqrt{\frac{\ln(\gamma)}{\gamma}}, & \gamma\gg 1,\end{cases}
\tag{C20}
$$

$$
S_{\rm tun}/N\sim\beta\begin{cases}1/\gamma+1.4, & \gamma\ll 1.\\ \sqrt{\frac{\ln(\gamma)}{\gamma}}, & \gamma\gg 1.\end{cases}
\tag{C21}
$$

as quoted in the main text.

4. Implications for interwire correlations

Using $\psi=(c,f)^T$ the generating functional at mean field level, but including fluctuations of the Goldstone modes is $Z=\prod_k Z_k$

$$
\begin{aligned}
Z_k[\eta] &= \int\mathcal{D}\psi_k e^{-\int d\tau\bar\psi_k[-\hat G^{-1}+i\mathcal{A}]\psi_k+\bar\psi_k U\eta_k+\bar\eta_k U^\dagger\psi_k}\\
&= e^{\int d\tau\bar\eta_k\hat G\eta_k+S[A_{2,3}]}.
\end{aligned}
\tag{C22}
$$

Here, U is the diagonal matrix introduced after Eq. (B2). Intersite correlator (obtained by differentiation with respect to η) thus contain averages like the following

$$\begin{aligned}\langle e^{iA_m(\tau)}e^{-iA_{m'}(0)}\rangle &= \mathrm{tr}[e^{-(\beta-\tau)H}e^{-iA_m}e^{-\tau H}e^{iA_{m'}}]\\ &\overset{T\to 0}{=} \sum_{\boldsymbol{p}}\int d^2x\int d^2x'\psi_0^*(\vec{x})e^{-iA_m(\vec{x})}\psi_{\vec{p}}(\vec{x})e^{-i\tau\epsilon_{\vec{p}}}\psi_{\vec{p}}^*(\vec{x}')e^{iA_{m'}(\vec{x}')}\psi_0(\vec{x}')\\ &= \delta_{mm'}e^{-i\epsilon_{-2\hat{e}_m/3}}.\end{aligned} \tag{C23}$$

We used the notation $\psi_{\vec{p}}(\vec{x})$ for eigenstates of $(-i\nabla_{\vec{x}})^2/(2m_x)$ with eigenenergy $\vec{p}^2/(2m_x)$. Thus, only intrasite terms survive.

5. Ordering of $\mathcal{O}_s = d_{abc}\hat{S}_1^a\hat{S}_2^b\hat{S}_3^c$.

For $t > t_c$ (i.e. in the 3CK phase), the effective action of Φ fluctuations can be obtained by expansion about the minimum of $\cos(\Phi)$ leading to

$$S[\Phi] = \int\frac{d\omega}{2\pi}\Phi(\omega)\Phi(-\omega)\left[\frac{\eta}{4\pi}|\omega| + \frac{M_\Phi}{2}\right] \tag{C24}$$

where $M_\Phi = N\beta T_K$. The correlator of phase fluctuations thus decays as

$$\langle\Phi(\tau)\Phi(0)\rangle \sim \int_0^\infty d\omega\frac{\cos(\omega\tau)}{\eta|\omega| + 2\pi M_\Phi} \sim -\frac{\eta\sin(2\pi M_\Phi\tau)}{(M_\Phi\tau)^2}, \tag{C25}$$

and therefore leads to long-range correlations

$$\langle\mathcal{O}_s(\tau)\mathcal{O}_s(0)\rangle \sim \frac{t^6}{T_{\mathrm{K}}^6}e^{-\frac{\eta\sin(2\pi M_\Phi\tau)}{(M_\Phi\tau)^2}} \to \frac{t^6}{T_{\mathrm{K}}^6}. \tag{C26}$$

Appendix D: Phase slips

Here we include phase slips of weight Γ and time τ_0 which is assumed to be smaller than all other time scales of the effective theory. We now consider a single kink in Φ with shift 2π, which is associated to an amplitude [88]

$$\mathcal{A}^{(0)}_{(-\tau/2,\Phi)\to(\tau/2,\Phi\pm 2\pi)} = \Gamma\int_{-\tau/2}^{\tau/2}d\tau_c. \tag{D1}$$

1. Instanton interactions

We consider the full partition function (generating functional) to second order in Γ.

$$Z[\eta] = Z_0[\eta] + \Gamma^2\sum_{\pm}\int_0^\beta d\tau_f\int_0^{\tau_i}d\tau_i Z_{2,\pm}[\eta;\tau_f,\tau_i], \tag{D2}$$

where a phaseslip (anti phase slip) is introduce at τ_i (τ_f) and the sum over $\pm$ indicates the direction of the slip. The partition function is

$$\begin{aligned}F &= -T\ln Z[0]\\ &\simeq \underbrace{-T\ln Z_0[0]}_{=F_0} - T\Gamma^2\sum_{\pm}\int_0^\beta d\tau_f\int_0^{\tau_i}d\tau_i\frac{Z_{2,\pm}[0;\tau_f,\tau_i]}{Z_0[0]}.\end{aligned} \tag{D3}$$

We use that, before and after a phase slip, h labels the same quantum states, however their energy has been shuffled around cyclically $\epsilon_h \to \epsilon_{h+1}$. We can thus express the partition function in the helicity basis, $Z_0[\eta] = \prod_h Z_{0,h}[\eta_k]$, $Z_{2,\pm}[\eta;\tau_f,\tau_i] = \prod_h Z_{2,\pm,h}[\eta_h;\tau_f,\tau_i]$ where (h index from now on suppressed unless explicitly restored)

$$Z_0[\eta] = \int\mathcal{D}[c,f]e^{-\int d\tau(\bar{c},\bar{f})[\partial_\tau + H_{\mathrm{MF}}](c,f)^T + \bar{\eta}f + \bar{f}\eta} \tag{D4a}$$

$$Z_2[\eta] = \int\mathcal{D}[c,f]e^{-\int d\tau(\bar{c},\bar{f})[\partial_\tau + H_{\mathrm{slips}}(\tau)](c,f)^T + \bar{\eta}f + \bar{f}\eta}, \tag{D4b}$$

and

$$H_{\mathrm{slips}}(\tau) = \begin{pmatrix}\epsilon(\boldsymbol{p}) & V\\ V & \lambda(\tau)\end{pmatrix} \tag{D4c}$$

where $\lambda(\tau) = \lambda + \delta\lambda\chi_{\tau_i,\tau_f}(\tau)$ and $\chi_{\tau_i,\tau_f}(\tau) = 1$ for $\tau_i < \tau < \tau_f$ and $\chi_{\tau_i,\tau_f}(\tau) = 0$, otherwise. Note that $\lambda = \lambda_h = \lambda - \epsilon_h$, for the ground state $\delta\lambda = 3t$, for one of the excited state $\delta\lambda = -3t$ and for the third state $\delta\lambda = 0$ ($k = \pm 2\pi/3$ are degenerate).

Thus, the instantons generate an x-ray edge problem in each helicity channel. We follow [89] and employ the long-time f-electron Green's function

$$G_f(\tau) \approx -\frac{g}{\tau}, \tag{D5}$$

with $g = \Delta/\pi(\Delta^2+\lambda^2)$ for the Kondo/resonant level problem. This leads to

$$S_{\mathrm{slips}}(\tau_f - \tau_i) = (\tau_f - \tau_i)\delta\lambda G_f(0,0^+) + \left(\frac{\delta_x}{\pi}\right)^2\ln\left(\frac{\tau_f - \tau_i}{\lambda}\right), \tag{D6}$$

where $\delta_x = -\arctan(\pi g\delta\lambda)$. The first (classical) term cancels upon taking the product of h, leaving only the logarithmic repulsion. This concludes the derivation of $\kappa = 2N(\delta_x/\pi)^2$, Eq. (19), as presented in the main text.

2. Infinite order resummation of phase slips

We now switch to the full resummation of phase slips. We consider an amplitude for $\Phi \to \Phi + N_\Phi 2\pi$ and denote n and $\bar{n}$ the number of kinks/antikinks (i.e. $n - \bar{n} = N_\Phi$) and their center of mass time $\tau_1,\dots\tau_{n+\bar{n}}$. Different instanton sequences correspond to the integral over these variables. Then the amplitude is

$$\mathcal{A}_{(0,\Phi)\to(\beta,\Phi+N_\Phi 2\pi)} = \sum_{n=0}^{\infty}\sum_{\bar{n}=0}^{\infty}\delta_{n-\bar{n},N_\Phi}\,\Gamma^{n+\bar{n}}\sum_{\substack{\text{perm. of}\\ \bar{n},n\text{ kinks}}}\Big\{\int_0^\beta d\tau_{n+\bar{n}}\cdots\int_0^{\tau_3}d\tau_2\int_0^{\tau_2}d\tau_1$$
$$\mathrm{tr}\big[e^{-\int_{\tau_{n+\bar{n}}}^{\beta}d\tau'\hat{H}_{\rm MF}(\Phi+N_\Phi 2\pi)}\ldots e^{-\int_{\tau_1}^{\tau_2}d\tau'\hat{H}_{\rm MF}(\Phi\pm 2\pi)}e^{-\int_{\tau_0}^{\tau_1}d\tau'\hat{H}_{\rm MF}(\Phi)}\big]\Big\}. \tag{D7}$$

In the second line, the ± refers to the sign of the first kink. We can now use that the Hamiltonian between two kinks is time independent and the evolution operator between two kinks is

$$\begin{aligned}\mathcal{T}e^{-\int_{\tau_l}^{\tau_{l+1}}d\tau'\hat{H}_{\rm MF}(\Phi+k2\pi)} &= \prod_{\Delta\tau}\big[1+\Delta\tau\hat{H}(\Phi+k2\pi)\big]\\ &= \prod_{\Delta\tau}\big(\tau_\Phi^k\,[1+\Delta\tau H(\Phi)]\,\tau_\Phi^{-k}\big)\\ &= \tau_\Phi^k\prod_{\Delta\tau}\big([1+\Delta\tau H(\Phi)]\big)\,\tau_\Phi^{-k}\\ &= \tau_\Phi^k\mathcal{T}[e^{-\int_{\tau_l}^{\tau_{l+1}}d\tau' H_{\rm MF}(\Phi)}]\tau_\Phi^{-k}.\end{aligned} \tag{D8}$$

Thus, a kink at time τ is represented by the operator insertion τ_Φ at time τ into the partition sum

$$\begin{aligned}\mathcal{A}_{(0,\Phi)\to(\beta,\Phi+N_\Phi 2\pi)} &= \sum_{n=0}^{\infty}\sum_{\bar{n}=0}^{\infty}\delta_{n-\bar{n},N_\Phi}\,\Gamma^{n+\bar{n}}\frac{(n+\bar{n})!}{n!\bar{n}!}\frac{1}{(n+\bar{n})!}\\ &\mathcal{T}\Big\{\int_0^\beta d\tau_n\cdots\int_0^\beta d\tau_1\int_0^\beta d\bar{\tau}_{\bar{n}}\cdots\int_0^\beta d\bar{\tau}_1\mathrm{tr}[\prod_{j=1}^{n}\prod_{\bar{j}=1}^{\bar{n}}\tau_\Phi(\tau_k)\tau_\Phi^{-1}(\bar{\tau}_{\bar{j}})e^{-\int_0^\beta d\tau\hat{H}_{\rm MF}}]\Big\}\\ &= \frac{1}{3}\sum_\theta e^{-i\theta N_\Phi}\mathrm{tr}[e^{\int_0^\beta d\tau\Gamma e^{i\theta}\tau_\Phi(\tau)}e^{\int_0^\beta d\tau\Gamma e^{-i\theta}\tau_\Phi^{-1}(\tau)}e^{-\int_0^\beta d\tau\hat{H}_{\rm MF}}].\end{aligned} \tag{D9}$$

We used the Fourier transform on ℓ^3 with periodic boundary conditions (i.e. with possible wavevectors $\theta = 0,\pm 2\pi/3$) such that $\sum_\theta e^{i\theta N} = 3\delta_{N,0}$ and $\sum_n e^{in\theta} = 3\delta_{\theta,0}$. Here, $\frac{(n+\bar{n})!}{n!\bar{n}!}$ is the number of possibilities to arrange the n upsteps if there are $n+\bar{n}$ steps in total. The factor $\frac{1}{(n+\bar{n})!}$ accounts for the fact that the integration domain has been increased from an explicitly time ordered $n+\bar{n}$ dimensional integral in Eq. (D7), to a $n+\bar{n}$ dimensional hypercube.

The total partition sum is given by (we use $\sum_{N_\Phi} e^{-iN_\Phi\theta} = 3\delta_{\theta,0}$ for $N_\Phi = 0,\pm 1$)

$$Z = \sum_{N_\phi}\mathcal{A}_{(0,\Phi)\to(\beta,\Phi+N_\Phi 2\pi)} = \mathrm{tr}\big[e^{-\beta[\hat{H}_{\rm MF}-\Gamma(\tau_\Phi+\tau_\Phi^{-1})]}\big] \tag{D10}$$

We now restore the matrix space of different vacua. In total we obtain

$$\begin{aligned}H_{\rm eff} = \sum_x&[-t_c c^\dagger_{\alpha m}(x)c_{\alpha m}(x+1)+h.c.-\mu c^\dagger_{\alpha m}(x)c_{\alpha m}(x)]\mathbf{1}_\Phi\\ &+[t\sigma_\Phi f^\dagger_{\alpha,m}f_{\alpha,m+1}+h.c.]+\lambda f^\dagger_{\alpha m}f_{\alpha m}\mathbf{1}_\Phi\\ &+[Vf^\dagger_{\alpha,m}c_{\alpha,m}+h.c.]\mathbf{1}_\Phi-\Gamma(\tau_\Phi+\tau_\Phi^{-1}).\end{aligned} \tag{D11}$$

This concludes the derivation of Eq. (17) of the main text.

3. Orthogonality catastrophe using bosonization

We start from the effective Hamiltonian derived in the previous section

$$H = H_0 + H_\Gamma, \qquad H_\Gamma = -\Gamma\hat{O}, \qquad \hat{O} = \tau_\Phi + \tau_\Phi^{-1}. \tag{D12}$$

We are going to treat this problem perturbatively to second order in Γ and diagonalize H_0 in the helicity h basis. Then, considering that $\lambda_h[\Phi]$ is different for $\Phi = -2\pi, 0, 2\pi$ we have

$$\begin{aligned}H_0 &= \sum_{\Phi=0}\sum_h|\Phi\rangle\,H_{0h}[\Phi]\,\langle\Phi|,\\ H_{0h}[\Phi] &= \begin{pmatrix}c\\ f\end{pmatrix}_h^\dagger\begin{pmatrix}\epsilon_c & V\\ V & \lambda_h[\Phi]\end{pmatrix}\begin{pmatrix}c\\ f\end{pmatrix}_h.\end{aligned} \tag{D13}$$

Note that c-electrons have another momentum k along the wires, which is implicit here. This problem as is, is

difficult to treat. We are forced to i) go to the scattering basis $\psi_{h\sigma}$ and ii) assume that the phase shift is independent of the energy, i.e. the electrons in scattering basis experience a potential scattering $\tilde{V}_h[\Phi]$ which depends on the flux Φ. In that case we can unfold the conduction electrons to right-movers only and write

$$H_{0h}[\Phi] = H_{0h} + \sqrt{2\pi}\tilde{V}_h[\Phi]\psi^\dagger_{h\sigma}(0)\psi_{h\sigma}(0),$$
$$H_{0h} = -iv_F\int dx\psi^\dagger_{h\sigma}\partial_x\psi_{h\sigma} \tag{D14}$$

where the relation between the potential scattering $\tilde{V}_h[\Phi]$ and the phase shift is shown below in Eq. (D18) and the factor of $\sqrt{2\pi}$ is introduced for future convenience. Next, we bosonize, i.e. express the fermions as

$$\psi_h(x) \sim e^{i\sqrt{2\pi}\varphi_h(x)},\ [\varphi_h(x),\varphi_{h'}(y)] = \frac{i}{2}\mathrm{sgn}(x-y)\delta_{hh'}. \tag{D15}$$

The Hamiltonian becomes

$$H_{0h}[\Phi] = H_{0h} + (\partial_x\varphi_h)\tilde{V}_h[\Phi],\ H_{0h} = \frac{v_F}{2}\int_0^\infty dx(\partial_x\varphi_h)^2. \tag{D16}$$

It is easy to see that the potential scattering term can be eliminated

$$H_{0h}[\Phi] \equiv \frac{v_F}{2}\int dx\Big\{\partial_x\varphi_h + \delta(x)\tilde{V}_h[\Phi]/v_F\Big\}^2,$$
$$\text{i.e.}\quad \varphi_h(x) \to \varphi_h(x) + \theta(x)\tilde{V}_h[\Phi]/v_F. \tag{D17}$$

By plugging this into $\psi \sim e^{i\sqrt{2\pi}\varphi}$ we can see that this corresponds to the phase shift

$$\psi_{out,h} = \psi_{in,h}e^{2i\delta_h}, \qquad \delta_h = \sqrt{\frac{\pi}{2}}\frac{\tilde{V}_h}{v_F} \tag{D18}$$

Each flux configuration corresponds to a different phase shift in a given helicity sector and these configurations are related to each other via the so-called Schotte-Schotte transformation [90]

$$U_h[\Phi,\Delta\Phi] = \exp\Big\{-i\varphi(0)\Big(\tilde{V}_h[\Phi+\Delta\Phi] - \tilde{V}_h[\Phi]\Big)/v_F\Big\}. \tag{D19}$$

Using the commutation relation of bosons and the fact that $e^{sX}Ye^{-sX} = Y + s[X,Y]$, for $[X,Y]$ c-number, we can check that

$$H_{0h}[\Phi+\Delta\Phi] = U^\dagger_h[\Phi,\Delta\Phi]H_{0h}[\Phi]U_h[\Phi,\Delta\Phi] \tag{D20}$$
$$= H_{0h} + (\partial_x\varphi)\tilde{V}_h[\Phi]$$
$$- i[\tilde{V}(\Phi+\Delta\Phi) - \tilde{V}(\Phi)]\int_x \partial_x\varphi[\varphi(0),\partial_x\varphi]$$
$$= H_{0h} + \tilde{V}[\Phi+\Delta\Phi](\partial_x\varphi)|_{x=0}. \tag{D21}$$

Going to interaction picture w.r.t. H_0 and expanding the partition function in Γ we have

$$Z/Z_0 = \langle T_\tau e^{-\int_{-1/2T}^{1/2T}d\tau H_\Gamma(\tau)}\rangle_0$$
$$= 1 + \frac{\Gamma^2}{2}\int d\tau_1 d\tau_2\,\langle T_\tau e^{\tau_1 H_0}\hat{O}e^{(\tau_2-\tau_1)H_0}\hat{O}e^{-\tau_2 H_0}\rangle_0$$
$$= 1 + \frac{\Gamma^2}{2}\int d\tau_1 d\tau_2\,\langle T_\tau e^{(\tau_1-\tau_2)H_0}e^{(\tau_2-\tau_1)\hat{O}H_0\hat{O}}\rangle_0$$
$$= 1 + \frac{\Gamma^2}{2}\sum_\Phi\sum_{\alpha=\pm1}\int d\tau_1 d\tau_2\prod_h$$
$$\times\,\langle T_\tau e^{(\tau_1-\tau_2)H_{0h}[\Phi]}e^{(\tau_2-\tau_1)H_{0h}[\Phi+2\pi\alpha]}\rangle_0 \tag{D22}$$

where $\hat{O} = \tau^{+1} + \tau^{-1}$, we used that the linear-in-Γ term vanishes due to trace and use the cyclic property of the trace with the Boltzmann factor $e^{-\beta H_0}/Z_0$ to shuffle the time-evolutions. Using Eq. (D20):

$$e^{\tau H_{0h}[\Phi+\Delta\Phi]} = U^\dagger_h[\Phi,\Delta\Phi]e^{\tau H_{0h}[\Phi]}U_h[\Phi,\Delta\Phi] \tag{D23}$$

we can write

$$\langle T_\tau e^{-\Delta\tau H_{0h}[\Phi]}U^\dagger_h[\Phi,\Delta\Phi]e^{\tau H_{0h}[\Phi]}U_h[\Phi,\Delta\Phi]\rangle_0$$
$$= \langle T_\tau U^\dagger_h[\Phi,\Delta\Phi;\tau]U_h[\Phi,\Delta\Phi]\rangle_0 \tag{D24}$$
$$= \langle T_\tau e^{i\varphi(\tau)\Delta V_h[\Phi,\Delta\Phi]/v_F}e^{-i\varphi(0)\Delta V_h[\Phi,\Delta\Phi]/v_F}\rangle$$
$$\sim |\tau|^{-\frac{(\Delta\tilde{V}_h[\Phi,\Delta\Phi])^2}{2\pi v_F^2}}$$

where we used that

$$\langle e^{i\gamma\varphi(\tau)}e^{-i\gamma\varphi(0)}\rangle = \frac{1}{|\tau|^{\gamma^2/2\pi}}. \tag{D25}$$

As a reminder, $\Delta\tilde{V}_h$ can be related to the phase shift

$$\Delta\tilde{V}_h[\Phi,\Delta\Phi] \equiv \tilde{V}_h[\Phi+\Delta\Phi] - \tilde{V}_h[\Phi]$$
$$= v_F\sqrt{\frac{2}{\pi}}\Big(\delta_h[\Phi+\Delta\Phi] - \delta_h[\Phi]\Big) \tag{D26}$$

which leads to

$$Z/Z_0 = 1 + \frac{1}{T}\Gamma^2\sum_\Phi\sum_{\alpha=\pm1}\int_{-1/2T}^{1/2T}d\Delta\tau\,|\Delta\tau|^{-\kappa},$$
$$\kappa = \sum_h(\delta_h[\Phi+\Delta\Phi]/\pi - \delta_h[\Phi]/\pi)^2. \tag{D27}$$

Up to subleading terms in small t (which are not important near the transition), this exactly reproduces Eq. (D6). The time-integral leads to

$$Z/Z_0 = 1 + \mathcal{C}'\Gamma^2T^{\kappa-2} \tag{D28}$$

where $\mathcal{C}'$ is a constant. The corrections to free energy $F_0 = -T\log Z_0$ is

$$F - F_0 = -\mathcal{C}'\Gamma^2T^{\kappa-1}. \tag{D29}$$

4. $\langle\sigma_\Phi(\tau)\sigma_\Phi(0)\rangle$ correlation function

In this section we compute the correlator $\langle\sigma_\Phi(\tau)\sigma_\Phi(0)\rangle$ which is related to the order parameter $\langle\mathcal{O}_s(\tau)\mathcal{O}_s(0)\rangle$ or $\langle\Phi(\tau)\Phi(\tau)\rangle$ in the paper, within the $t-\Gamma$ Hamiltonian $H = H_0 + H_\Gamma$. In the $\Gamma/t \gg 1$ regime (FL phase) this is exponentially decaying. This can be seen easily in a basis in which the $-\Gamma O$ term is diagonal. In the limit of large Γ, we can use a unitary transformation U_O to diagonalize O

$$O = \tau_\Phi + \tau_\Phi^{-1} = \begin{pmatrix} 0 & 1 & 1 \\ 1 & 0 & 1 \\ 1 & 1 & 0 \end{pmatrix} \to U_O^\dagger O U_O = \begin{pmatrix} -1 & & \\ & -1 & \\ & & 2 \end{pmatrix} \tag{D30}$$

and go to the interaction picture w.r.t. $-\Gamma\tau^x$. In this picture $\sigma(\tau)$ is time-dependent and is given by

$$\rho_\Gamma = \frac{e^{-\Gamma/T}}{2e^{-\Gamma/T} + e^{2\Gamma/T}} \begin{pmatrix} 1 & & \\ & 1 & \\ & & e^{3\Gamma/T} \end{pmatrix} \to \begin{pmatrix} 0 & & \\ & 0 & \\ & & 1 \end{pmatrix},$$
$$\sigma_\Gamma(\tau) = \frac{\omega^2}{2} \begin{pmatrix} 1 & i & -x^{-1}\sqrt{2} \\ i & -1 & ix^{-1}\sqrt{2} \\ -x\sqrt{2} & ix\sqrt{2} & 0 \end{pmatrix}, \tag{D31}$$

in terms of $x = e^{3\tau\Gamma}$. With this density matrix $\mathrm{tr}[\rho_\Gamma O] = o_{33}$. Therefore to leading order in tunnelling t,

$$\langle\sigma_\Gamma\rangle = \langle T_\tau\sigma_\Gamma(\tau)\sigma_\Gamma(0)\rangle = 0,$$
$$\langle T_\tau\sigma_\Gamma(\tau)\sigma_\Gamma^\dagger(0)\rangle = \langle T_\tau\sigma_\Gamma^\dagger(\tau)\sigma_\Gamma(0)\rangle = e^{-3|\tau|\Gamma}. \tag{D32}$$

This is the origin of the fact that t is irrelevant in the $\Gamma/t \gg 1$ regime, within $t-\Gamma$ Hamiltonian. In the opposite regime of $\Gamma/t \ll 1$, we can use the same technique as in previous section to compute the Since σ_Φ commutes with H_0, to zero order in Γ we have

$$\langle\sigma_\Phi(\tau)\sigma_\phi^\dagger(0)\rangle = \frac{1}{3}\mathrm{tr}[\sigma_\Phi\sigma_\phi^\dagger] = 1. \tag{D33}$$

To second order in Γ we have (we have neglected the disconnected part, since it does not depend on τ)

$$\langle\sigma_\Phi(\tau)\sigma_\phi^\dagger(0)\rangle =$$
$$1 + \Gamma^2\int_{-1/2T}^{1/2T} d\tau_1 d\tau_2\, \langle T_\tau\sigma_\Phi(\tau)\sigma_\Phi^\dagger(0)\hat{O}(\tau_1)\hat{O}(\tau_2)\rangle \tag{D34}$$

We can divide the integration range into 6 configurations (assuming $\tau_1 > \tau_2$):

$$\theta_1 \equiv \theta(\tau_1 > \tau_2 > \tau > 0): \quad \sum_{\alpha\alpha'}\langle e^{\tau_1 H_0}\tau_\Phi^\alpha e^{(\tau_2-\tau_1)H_0}\tau_\Phi^{\alpha'} e^{-\tau_2 H_0}\sigma_\Phi\sigma_\Phi^\dagger\rangle = G(\Delta\tau) \tag{D35}$$
$$\theta_2 \equiv \theta(\tau > 0 > \tau_1 > \tau_2): \quad \sum_{\alpha\alpha'}\langle \sigma_\Phi\sigma_\Phi^\dagger e^{\tau_1 H_0}\tau_\Phi^\alpha e^{(\tau_2-\tau_1)H_0}\tau_\Phi^{\alpha'} e^{-\tau_2 H_0}\rangle = \omega G(\Delta\tau) \tag{D36}$$
$$\theta_3 \equiv \theta(\tau > \tau_1 > \tau_2 > 0): \quad \sum_{\alpha\alpha'}\langle \sigma_\Phi e^{\tau_1 H_0}\tau_\Phi^\alpha e^{(\tau_2-\tau_1)H_0}\tau_\Phi^{\alpha'} e^{-\tau_2 H_0}\sigma_\Phi^\dagger\rangle = G(\Delta\tau) \tag{D37}$$
$$\theta_4 \equiv \theta(\tau_1 > \tau > 0 > \tau_2): \quad \sum_{\alpha\alpha'}\langle e^{\tau_1 H_0}\tau_\Phi^\alpha e^{-\tau_1 H_0}\sigma_\Phi\sigma_\Phi^\dagger e^{\tau_2 H_0}\tau_\Phi^{\alpha'} e^{-\tau_2 H_0}\rangle = \bar{\omega} G(\Delta\tau) \tag{D38}$$
$$\theta_5 \equiv \theta(\tau > \tau_1 > 0 > \tau_2): \quad \sum_{\alpha\alpha'}\langle \sigma_\Phi e^{\tau_1 H_0}\tau_\Phi^\alpha e^{-\tau_1 H_0}\sigma_\Phi^\dagger e^{\tau_2 H_0}\tau_\Phi^{\alpha'} e^{-\tau_2 H_0}\rangle = G(\Delta\tau) \tag{D39}$$
$$\theta_6 \equiv \theta(\tau_1 > \tau > \tau_2 > 0): \quad \sum_{\alpha\alpha'}\langle e^{\tau_1 H_0}\tau_\Phi^\alpha e^{-\tau_1 H_0}\sigma_\Phi e^{\tau_2 H_0}\tau_\Phi^{\alpha'} e^{-\tau_2 H_0}\sigma_\Phi^\dagger\rangle = G(\Delta\tau) \tag{D40}$$

Here, $\alpha, \alpha' = +1, -1$ and we have used the $\sigma_\Phi\tau_\Phi = \omega\tau_\Phi\sigma_\Phi$ and similar commutation relations to eliminate σ_Φ and τ_Φ and express the correlators in terms of a single correlator

$(\Delta\tau \equiv \tau_1 - \tau_2)$

$$G(\Delta\tau) = \sum_\alpha\sum_\Phi\prod_h\langle e^{\Delta\tau H_0[\Phi]}e^{-\Delta\tau H_0[\Phi+2\pi\alpha]}\rangle, \tag{D41}$$

which is the correlator was computed in the previous section The integration over these ranges appear with a integrand that is only a function of $\tau_1 - \tau_2$. Denoting,

$$I_i \equiv \int d\tau_1 d\tau_2 \theta_i G(\tau_1 - \tau_2) \tag{D42}$$

we have typical integrals of the form

$$I \sim \tau \int_0^\tau d\Delta\tau G(\Delta\tau), \qquad G(\Delta\tau) \sim |\Delta\tau|^{-\kappa} \tag{D43}$$

in terms of κ defined before, which gives us

$$\langle \sigma_\Phi(\tau)\sigma_\Phi^\dagger(0)\rangle \sim 1 + \mathcal{C}''\Gamma^2\tau^{2-\kappa}. \tag{D44}$$

where $\mathcal{C}''$ is another constant. This demonstrates that the $\langle \sigma_\Phi(\tau)\sigma_\Phi(0)\rangle$ correlator disorders at the deconfinement quantum phase transition, defined by $\kappa = 2$.

[1] Lucile Savary and Leon Balents, "Quantum spin liquids: a review," Reports on Progress in Physics **80**, 016502 (2016).

[2] Yi Zhou, Kazushi Kanoda, and Tai-Kai Ng, "Quantum spin liquid states," Rev. Mod. Phys. **89**, 025003 (2017).

[3] Xiao-Gang Wen, "Colloquium: Zoo of quantum-topological phases of matter," Rev. Mod. Phys. **89**, 041004 (2017).

[4] T. Senthil, Ashvin Vishwanath, Leon Balents, Subir Sachdev, and Matthew P. A. Fisher, " Deconfined Quantum Critical Points," Science **303**, 1490–1494 (2004).

[5] P. W. Anderson, Science **235**, 1196–1198 (1987).

[6] Y. Kurosaki, Y. Shimizu, K. Miyagawa, K. Kanoda, and G. Saito, "Mott transition from a spin liquid to a Fermi liquid in the spin-frustrated organic conductor κ–$(ET)_2Cu_2(CN)_3$," Phys. Rev. Lett. **95**, 177001 (2005).

[7] Satoshi Yamashita, Yasuhiro Nakazawa, Masaharu Oguni, Yugo Oshima, Hiroyuki Nojiri, Yasuhiro Shimizu, Kazuya Miyagawa, and Kazushi Kanoda, "Thermodynamic properties of a spin-1/2 spin-liquid state in a κ-type organic salt," Nature Physics **4**, 459 (2008).

[8] Piers Coleman, Yashar Komijani, and Elio J. König, "Triplet resonating valence bond state and superconductivity in Hund's metals," Phys. Rev. Lett. **125**, 077001 (2020).

[9] A Dönni, G Ehlers, H Maletta, P Fischer, H Kitazawa, and M Zolliker, "Geometrically frustrated magnetic structures of the heavy-Fermion compound cepdal studied by powder neutron diffraction," Journal of Physics: Condensed Matter **8**, 11213 (1996).

[10] Akito Sakai, Stefan Lucas, Philipp Gegenwart, Oliver Stockert, Hilbert v. Löhneysen, and Veronika Fritsch, "Signature of frustrated moments in quantum critical $CePd_{1-x}Ni_xAl$," Phys. Rev. B **94**, 220405 (2016).

[11] A Ribak, R Majlin Skiff, M Mograbi, PK Rout, MH Fischer, J Ruhman, K Chashka, Y Dagan, and A Kanigel, "Chiral superconductivity in the alternate stacking compound 4Hb-TaS_2," arXiv:1905.02225 (2019).

[12] Soudabeh Mashhadi, Youngwook Kim, Jeongwoo Kim, Daniel Weber, Takashi Taniguchi, Kenji Watanabe, Noejung Park, Bettina Lotsch, Jurgen H. Smet, Marko Burghard, and Klaus Kern, "Spin-split band hybridization in graphene proximitized with α-RuCl3 nanosheets," Nano Letters **19**, 4659–4665 (2019), pMID: 31241971.

[13] Piers Coleman, "$\frac{1}{N}$ expansion for the Kondo lattice," Phys. Rev. B **28**, 5255–5262 (1983).

[14] Daniel P. Arovas and Assa Auerbach, "Functional integral theories of low-dimensional quantum Heisenberg models," Phys. Rev. B **38**, 316–332 (1988).

[15] Alexander M Polyakov, "Quark confinement and topology of gauge theories," Nuclear Physics B **120**, 429–458 (1977).

[16] Michael Hermele, T. Senthil, Matthew P. A. Fisher, Patrick A. Lee, Naoto Nagaosa, and Xiao-Gang Wen, "Stability of $U(1)$ spin liquids in two dimensions," Phys. Rev. B **70**, 214437 (2004).

[17] Sung-Sik Lee, "Stability of the U(1) spin liquid with a spinon Fermi surface in $2+1$ dimensions," Phys. Rev. B **78**, 085129 (2008).

[18] Xue-Yang Song, Chong Wang, Ashvin Vishwanath, and Yin-Chen He, "Unifying description of competing orders in two-dimensional quantum magnets," Nature communications **10**, 1–12 (2019).

[19] Xiao Yan Xu, Yang Qi, Long Zhang, Fakher F. Assaad, Cenke Xu, and Zi Yang Meng, "Monte Carlo study of lattice compact quantum electrodynamics with fermionic matter: The parent state of quantum phases," Phys. Rev. X **9**, 021022 (2019).

[20] Éric Dupuis, M. B. Paranjape, and William Witczak-Krempa, "Transition from a dirac spin liquid to an antiferromagnet: Monopoles in a QED_3-Gross-Neveu theory," Phys. Rev. B **100**, 094443 (2019).

[21] T Senthil, Subir Sachdev, and Matthias Vojta, "Fractionalized Fermi liquids," Phys. Rev. Lett. **90**, 216403 (2003).

[22] Yashar Komijani and Piers Coleman, "Model for a ferromagnetic quantum critical point in a 1d Kondo lattice," Phys. Rev. Lett. **120**, 157206 (2018).

[23] Yashar Komijani and Piers Coleman, "Emergent critical charge fluctuations at the Kondo breakdown of heavy Fermions," Phys. Rev. Lett. **122**, 217001 (2019).

[24] Ady Stern and Netanel H Lindner, "Topological quantum computationfrom basic concepts to first experiments," Science **339**, 1179–1184 (2013).

[25] Ph. Nozières and A. Blandin, " Kondo effect in real metals," J. Phys. France **41**, 193–211 (1980).

[26] N. Andrei and C. Destri, "Solution of the multichannel Kondo problem," Phys. Rev. Lett. **52**, 364–367 (1984).

[27] AM Tsvelick and PB Wiegmann, "Solution of the n-channel Kondo problem (scaling and integrability)," Zeitschrift für Physik B Condensed Matter **54**, 201–206 (1984).

[28] Ian Affleck and Andreas W. W. Ludwig, "Exact critical theory of the two-impurity Kondo model," Phys. Rev. Lett. **68**, 1046–1049 (1992).

[29] P. Coleman, L. B. Ioffe, and A. M. Tsvelik, "Simple formulation of the two-channel Kondo model," Phys. Rev. B **52**, 6611–6627 (1995).

[30] Kevin Ingersent, Andreas WW Ludwig, and Ian Affleck, "Kondo screening in a magnetically frustrated nanostructure: exact results on a stable non-Fermi-liquid phase," Phys. Rev. Lett. **95**, 257204 (2005).

[31] K. Hattori and H. Tsunetsugu, "Non-Fermi liquid, unscreened scalar chirality, and parafermions in a frustrated tetrahedron anderson model," Phys. Rev. B **86**, 054421 (2012).

[32] Bence Lazarovits, Pascal Simon, Gergely Zarand, and Laszlo Szunyogh, "Exotic Kondo effect from magnetic trimers," Phys. Rev. Lett. **95**, 077202 (2005).

[33] Andrew K. Mitchell, Thomas F. Jarrold, and David E. Logan, "Quantum phase transition in quantum dot trimers," Phys. Rev. B **79**, 085124 (2009).

[34] Tathagata Chowdhury, Achim Rosch, and Ralf Bulla, "Competition between Kondo and Kitaev physics in Kitaev clusters coupled to a Fermionic bath," arXiv:1910.14136 (2019).

[35] P. Zinn-Justin and N. Andrei, "The generalized multichannel Kondo model: Thermodynamics and fusion equations," Nuclear Physics B **528**, 648–682 (1998).

[36] Pedro L. S. Lopes, Ian Affleck, and Eran Sela, "Anyons in multichannel Kondo systems," ArXiv:1911.06336 (2019).

[37] Yashar Komijani, "Isolating Kondo anyons for topological quantum computation," Phys. Rev. B **101**, 235131 (2020).

[38] Michel Ferrero, Lorenzo De Leo, Philippe Lecheminant, and Michele Fabrizio, "Strong correlations in a nutshell," Journal of Physics: Condensed Matter **19**, 433201 (2007).

[39] Aline Ramires and Piers Coleman, "Supersymmetric approach to heavy fermion systems," Phys. Rev. B **93**, 035120 (2016).

[40] We here use the word "spinon" synonymously with "Abrikosov fermion". Ref. [91] contains a more careful terminological discussion which illustrates that the Abrikosov fermion (called "Spinon" with capital "S" there), is not necessarily equivalent with the fermionic low-energy degrees of freedom of a spin liquid ("spinons" with lower case "s").

[41] J. Brad Marston and Ian Affleck, "Large-n limit of the hubbard-Heisenberg model," Phys. Rev. B **39**, 11538–11558 (1989).

[42] B. A. Jones, C. M. Varma, and J. W. Wilkins, "Low-temperature properties of the two-impurity Kondo hamiltonian," Phys. Rev. Lett. **61**, 125–128 (1988).

[43] B. A. Jones, B. G. Kotliar, and A. J. Millis, "Mean-field analysis of two antiferromagnetically coupled anderson impurities," Phys. Rev. B **39**, 3415–3418 (1989).

[44] Andrew K. Mitchell, Eran Sela, and David E. Logan, "Two-channel Kondo physics in two-impurity Kondo models," Phys. Rev. Lett. **108**, 086405 (2012).

[45] T. Senthil, Matthias Vojta, and Subir Sachdev, "Weak magnetism and non-Fermi liquids near heavy-fermion critical points," Phys. Rev. B **69**, 035111 (2004).

[46] I. Paul, C. Pépin, and M. R. Norman, "Kondo breakdown and hybridization fluctuations in the Kondo-Heisenberg lattice," Phys. Rev. Lett. **98**, 026402 (2007).

[47] Matthias Vojta, "Orbital-selective mott transitions: Heavy fermions and beyond," Journal of Low Temperature Physics **161**, 203–232 (2010).

[48] Victor Drouin-Touchette, Elio J König, Yashar Komijani, and Piers Coleman, "Emergent moments in a Hund's impurity," arXiv:2101.10332 (2021).

[49] Yu. B. Kudasov and V. M. Uzdin, "Kondo state for a compact cr trimer on a metallic surface," Phys. Rev. Lett. **89**, 276802 (2002).

[50] Bruce C Paul and Kevin Ingersent, "Frustration-induced non-fermi-liquid behavior in a three-impurity Kondo model," arXiv preprint cond-mat/9607190 (1996).

[51] Fabian Eickhoff and Frithjof B. Anders, "Strongly correlated multi-impurity models: The crossover from a single-impurity problem to lattice models," Phys. Rev. B **102**, 205132 (2020).

[52] Andrew K. Mitchell, Thomas F. Jarrold, and David E. Logan, "Quantum phase transition in quantum dot trimers," Phys. Rev. B **79**, 085124 (2009).

[53] P. P. Baruselli, R. Requist, M. Fabrizio, and E. Tosatti, "Ferromagnetic Kondo effect in a triple quantum dot system," Phys. Rev. Lett. **111**, 047201 (2013).

[54] Krzysztof P Wójcik, Ireneusz Weymann, and Johann Kroha, "Magnetic Kondo regimes in a frustrated half-filled trimer," Physical Review B **102**, 045144 (2020).

[55] AM Tsvelick, "The thermodynamics of multichannel Kondo problem," Journal of Physics C: Solid State Physics **18**, 159 (1985).

[56] I Affleck, "Lectures given at the xxxvth Cracow school of theoretical physics, Zakopane, Poland, june 1995," Acta Polon. B **26**, 1869 (1995).

[57] Andrés Jerez, Natan Andrei, and Gergely Zaránd, "Solution of the multichannel Coqblin-Schrieffer impurity model and application to multilevel systems," Phys. Rev. B **58**, 3814–3841 (1998).

[58] P. Coleman, J. B. Marston, and A. J. Schofield, "Transport anomalies in a simplified model for a heavy-electron quantum critical point," Phys. Rev. B **72**, 245111 (2005).

[59] Xiao-Gang Wen, "Quantum orders and symmetric spin liquids," Phys. Rev. B **65**, 165113 (2002).

[60] Elio J König, Piers Coleman, and Alexei M Tsvelik, "Soluble limit and criticality of fermions in $\mathbb{Z}_2$ gauge theories," arXiv:1912.11106 (2019).

[61] Ian Affleck and Andreas W. W. Ludwig, "Universal noninteger "ground-state degeneracy" in critical quantum systems," Phys. Rev. Lett. **67**, 161–164 (1991).

[62] Onuttom Narayan and B Sriram Shastry, "The 2d coulomb gas on a 1d lattice," Journal of Physics A: Mathematical and General **32**, 1131–1146 (1999).

[63] AO Caldeira and Anthony J Leggett, "Quantum tunnelling in a dissipative system," Annals of physics **149**, 374–456 (1983).

[64] C. L. Kane and Matthew P. A. Fisher, "Transport in a one-channel Luttinger liquid," Phys. Rev. Lett. **68**, 1220–1223 (1992).

[65] J Villain, "A magnetic analogue of stereoisomerism: application to helimagnetism in two dimensions," Journal de Physique **38**, 385–391 (1977).

[66] Eduardo Fradkin and Leonard Susskind, "Order and disorder in gauge systems and magnets," Phys. Rev. D **17**, 2637–2658 (1978).

[67] Premala Chandra, Piers Coleman, and AI Larkin, "Ising transition in frustrated Heisenberg models," Phys. Rev. Lett. **64**, 88 (1990).

[68] Rafael M Fernandes, Peter P Orth, and Jörg Schmalian, "Intertwined vestigial order in quantum materials: Nematicity and beyond," Annual Review of Condensed Matter Physics **10**, 133–154 (2019).

[69] Subir Sachdev, "Topological order, emergent gauge fields, and fermi surface reconstruction," Reports on Progress in

Physics **82**, 014001 (2018).
[70] B. Béri and N. R. Cooper, "Topological Kondo effect with Majorana Fermions," Phys. Rev. Lett. **109**, 156803 (2012).
[71] E. J. König, Piers Coleman, and A. M. Tsvelik, "Spin magnetometry as a probe of stripe superconductivity in twisted bilayer graphene," Phys. Rev. B **102**, 104514 (2020).
[72] Antoine Georges, Gabriel Kotliar, Werner Krauth, and Marcelo J. Rozenberg, "Dynamical mean-field theory of strongly correlated fermion systems and the limit of infinite dimensions," Rev. Mod. Phys. **68**, 13–125 (1996).
[73] Thomas Maier, Mark Jarrell, Thomas Pruschke, and Matthias H. Hettler, "Quantum cluster theories," Rev. Mod. Phys. **77**, 1027–1080 (2005).
[74] Anna Keselman, Bela Bauer, Cenke Xu, and Chao-Ming Jian, "Emergent Fermi surface in a triangular-lattice SU(4) quantum antiferromagnet," Phys. Rev. Lett. **125**, 117202 (2020).
[75] Alexander Wietek, Riccardo Rossi, Fedor Simkovic IV, Marcel Klett, Philipp Hansmann, Michel Ferrero, E Miles Stoudenmire, Thomas Schäfer, and Antoine Georges, "Mott insulating states with competing orders in the triangular lattice hubbard model," arXiv preprint arXiv:2102.12904 (2021).
[76] Cenke Xu and Leon Balents, "Topological superconductivity in twisted multilayer graphene," Phys. Rev. Lett. **121**, 087001 (2018).
[77] M Haule, EY Andrei, and K Haule, "The mott-semiconducting state in the magic angle bilayer graphene," arXiv:1901.09852 (2019).
[78] Swapan K. Pati, Rajiv R. P. Singh, and Daniel I. Khomskii, "Alternating spin and orbital dimerization and spin-gap formation in coupled spin-orbital systems," Phys. Rev. Lett. **81**, 5406–5409 (1998).
[79] Y. Q. Li, Michael Ma, D. N. Shi, and F. C. Zhang, "SU(4) theory for spin systems with orbital degeneracy," Phys. Rev. Lett. **81**, 3527–3530 (1998).
[80] Y Tokura and N Nagaosa, "Orbital physics in transition-metal oxides," science **288**, 462–468 (2000).
[81] Masahiko G. Yamada, Masaki Oshikawa, and George Jackeli, "Emergent SU(4) symmetry in $\alpha-\mathrm{zrcl}_3$ and crystalline spin-orbital liquids," Phys. Rev. Lett. **121**, 097201 (2018).
[82] Alexey Vyacheslavovich Gorshkov, M Hermele, V Gurarie, C Xu, Paul S Julienne, J Ye, Peter Zoller, Eugene Demler, Mikhail D Lukin, and AM Rey, "Two-orbital SU (n) magnetism with ultracold alkaline-earth atoms," Nature physics **6**, 289–295 (2010).
[83] Francesco Scazza, Christian Hofrichter, Moritz Höfer, PC De Groot, Immanuel Bloch, and Simon Fölling, "Observation of two-orbital spin-exchange interactions with ultracold SU (n)-symmetric fermions," Nature Physics **10**, 779–784 (2014).
[84] AJ Keller, S Amasha, I Weymann, CP Moca, IG Rau, JA Katine, Hadas Shtrikman, G Zaránd, and D Goldhaber-Gordon, "Emergent SU (4) Kondo physics in a spin–charge-entangled double quantum dot," Nature Physics **10**, 145 (2014).
[85] M. Seo, H. K. Choi, S.-Y. Lee, N. Kim, Y. Chung, H.-S. Sim, V. Umansky, and D. Mahalu, "Charge frustration in a triangular triple quantum dot," Phys. Rev. Lett. **110**, 046803 (2013).
[86] Z Iftikhar, A Anthore, AK Mitchell, FD Parmentier, U Gennser, A Ouerghi, A Cavanna, C Mora, P Simon, and F Pierre, "Tunable quantum criticality and super-ballistic transport in a charge Kondo circuit," Science **360**, 1315–1320 (2018).
[87] Piers Coleman, *Introduction to many-body physics* (Cambridge University Press, 2015).
[88] A I Vaĭnshteĭn, Valentin I Zakharov, Viktor A Novikov, and Mikhail A Shifman, "ABC of instantons," Soviet Physics Uspekhi **25**, 195–215 (1982).
[89] Alexander O Gogolin, Alexander A Nersesyan, and Alexei M Tsvelik, *Bosonization and strongly correlated systems* (Cambridge university press, 2004).
[90] I. Affleck and A. W. W. Ludwig, "The Fermi edge singularity and boundary condition changing operators," Journal of Physics A: Mathematical and General **27**, 5375–5392 (1994).
[91] T Senthil and Matthew PA Fisher, "Fractionalization and confinement in the U (1) and $\mathbb{Z}2$ gauge theories of strongly correlated systems," Journal of Physics A: Mathematical and General **34**, L119 (2001).